nature portfolio

https://doi.org/10.1038/s41557-022-01025-9

Supplementary information

Lewis acid-assisted reduction of nitrite to nitric and nitrous oxides via the elusive nitrite radical dianion

In the format provided by the authors and unedited

Supplementary Information for:

Lewis Acid-Assisted Reduction of Nitrite to Nitric and Nitrous Oxides via the Elusive Nitrite Radical Dianion

Valiallah Hosseininasab,[1] Ida M. DiMucci,[2] Pokhraj Ghosh,[1,5] Jeffery. A. Bertke,[1] Siddarth Chandrasekharan,[2] Charles J. Titus,[3] Dennis Nordlund,[4] Jack H. Freed,[2] Kyle. M. Lancaster,[2,*] and Timothy. H. Warren,[1,5,*]

Affiliations:

[1] Department of Chemistry, Georgetown University, Box 571227, Washington, DC 20057, United States.

[2] Department of Chemistry and Chemical Biology, Cornell University, 122 Baker Laboratory, Ithaca, New York 14853, United States.

[3] Department of Physics, Stanford University, Stanford, California 94305, USA

[4] Stanford Synchrotron Radiation Lightsource, SLAC National Accelerator Laboratory, Menlo Park, California 94025, USA

[5] Department of Chemistry, Michigan State University, East Lansing, MI 48824, USA.

Corresponding authors email:

kml236@cornell.edu (K.M.L)
thw@georgetown.edu (T.H.W.)

1. General Instrumentation and Physical Methods

All experiments were carried out under dry nitrogen atmosphere by utilizing MBraun gloveboxes and/or standard Schlenk techniques unless otherwise mentioned. ^{1}H, ^{19}F, $^{13}C\{^{1}H\}$, ^{15}N and ^{11}B NMR spectra were recorded on a Varian 400 MHz spectrometer at room temperature unless otherwise noted. The chemical shift (δ) values for ^{1}H, and $^{13}C\{^{1}H\}$ are expressed in ppm relative to tetramethylsilane while the chemical shift (δ) values for ^{19}F, ^{15}N and ^{11}B NMR are expressed in ppm relative to C_6H_5F, $^{15}NH_3$ and boric acid, respectively. The residual ^{1}H signal of deuterated solvent served as an internal standard for ^{1}H and $^{13}C\{^{1}H\}$ NMRs whereas the residual ^{19}F signal of C_6H_5F served as an internal standard for ^{19}F NMR. Elemental analyses were performed on a Perkin-Elmer PE2400 micro-analyzer at Georgetown University. UV-vis spectra were recorded on Agilent 8454 Diode Array spectrometer equipped with stirrer and Unisoku USP-203 cryostat for variable temperature experiments. The molar extinction coefficients of different isolated complexes were determined from Beer's law plots (absorbance *vs* concentration) with at least four different concentrations. IR spectra (with spectral resolution of 2 cm^{-1}) were collected on an ATR spectrometer. Details for X-ray crystallography appear in Section 14.

2. Materials

All chemicals were purchased from common vendors (e.g. Sigma-Aldrich, Acros Organics, Strem Chemicals, TCI) and used without further purification unless otherwise mentioned. Tris(pentafluorophenyl)borane ($B(C_6F_5)_3$) was obtained from Boulder Scientific Company and used without further purification. Molecular sieves (4A, 4-8 mesh beads) were obtained from Fisher Scientific and were activated prior to use *in vacuo* at 200 °C for 24 h. Extra dry solvents (≥99.5%) with Acroseal® and deuterated solvents were purchased from Acros Organics and Cambridge Isotope Laboratories, respectively. Both anhydrous and deuterated solvents were sparged with nitrogen and stored over activated 4A molecular sieves under a nitrogen atmosphere. $Ag^{15}NO_2$ was prepared from commercially available $Na^{15}NO_2$ based on the previously reported procedure.[1,2]

3. Synthesis and Characterization of $[Cp^*_2Co][NO_2]$ (1)

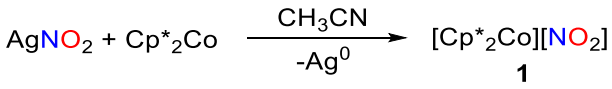

Scheme 1. Synthesis of $[Cp^*_2Co][NO_2]$ (**1**)

Cp^*_2Co (0.300 g, 0.910 mmol) in acetonitrile was directly added to a solution of $AgNO_2$ (0.140 g, 0.910 mmol) in acetonitrile (*ca.* 6 mL). The solution was stirred for 2 h at RT and the resultant dark brown solution was filtered through Celite and then concentrated to dryness under vacuum overnight to obtain a yellow solid. The yellow solid was dissolved in a mixture of CH_2Cl_2 / C_6H_5F (ca. 6 mL; 2/4) and crystalized at -40 °C by layering with pentane to obtain X-ray quality crystals (0.250 g, 0.665 mmol) in 73% yield. **1-^{15}N** was prepared similarly from $Ag^{15}NO_2$.

^{1}H NMR (400 MHz, CD_2Cl_2): δ 1.73 (s, 30 H, CH_3) (Figure S1);

$^{13}C\{^1H\}$ NMR (100 MHz, CD_2Cl_2): δ 94.63, 8.48;

^{15}N NMR (41 MHz, CD_2Cl_2): δ 611.66 (**1-^{15}N**);

FT-IR (cm^{-1}): 1226 ν(^{14}NO) (sym); 1344 ν(^{14}NO) (asym); 1201 ν(^{15}NO) (sym); 1317 ν(^{15}NO) (asym); Hooke's law predicts $^{15N/14N}\Delta\nu$ = 24 $cm^{-1}$and $^{15N/14N}\Delta\nu$ = 26, respectively (Figure S2).The IR spectra were taken as a thin film by evaporating a dichloromethane solution of **1** on a KBr window. Anal.Calcd for $C_{20}H_{30}CoNO_2$: C, 63.99; H, 8.06; N, 3.73. Found: C, 64.15; H, 7.90; N, 3.89.

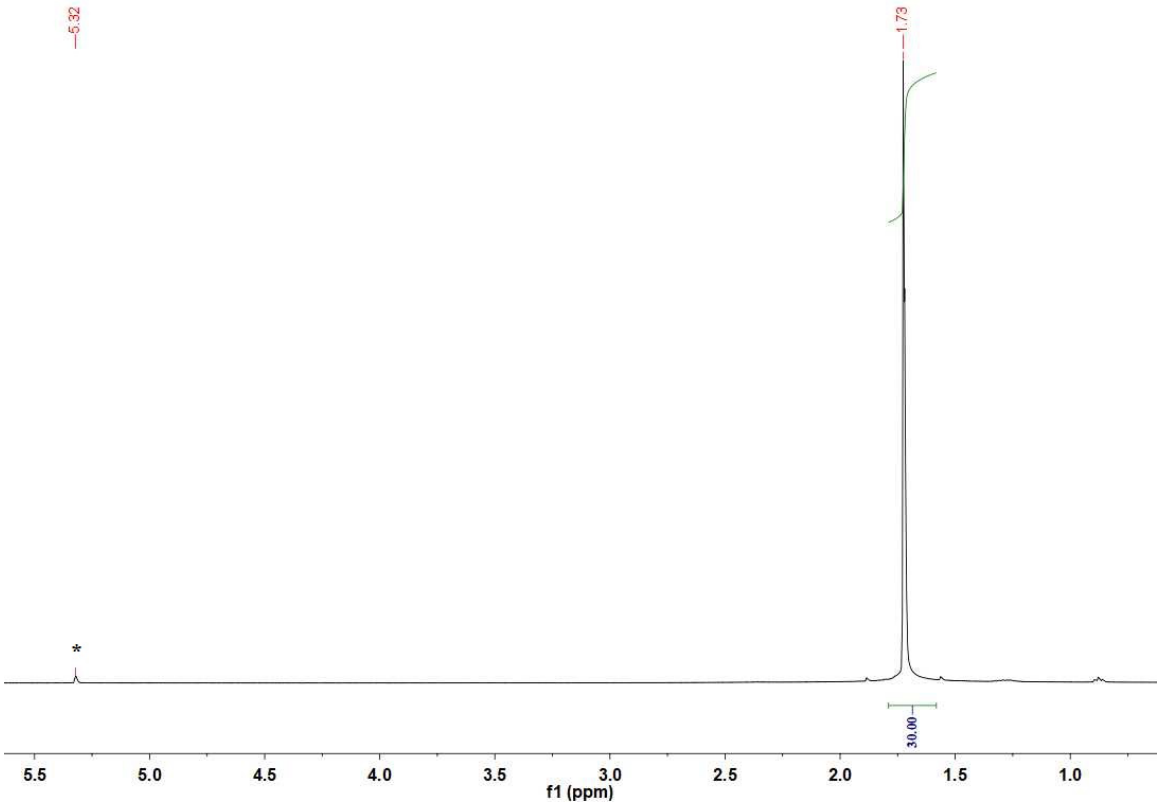

Figure 1. ^{1}H NMR spectrum (400 MHz, CD_2Cl_2) of $[Cp^*_2Co][NO_2]$ (**1**). The resonance marked with (*) belongs to residual proton impurities of CD_2Cl_2.

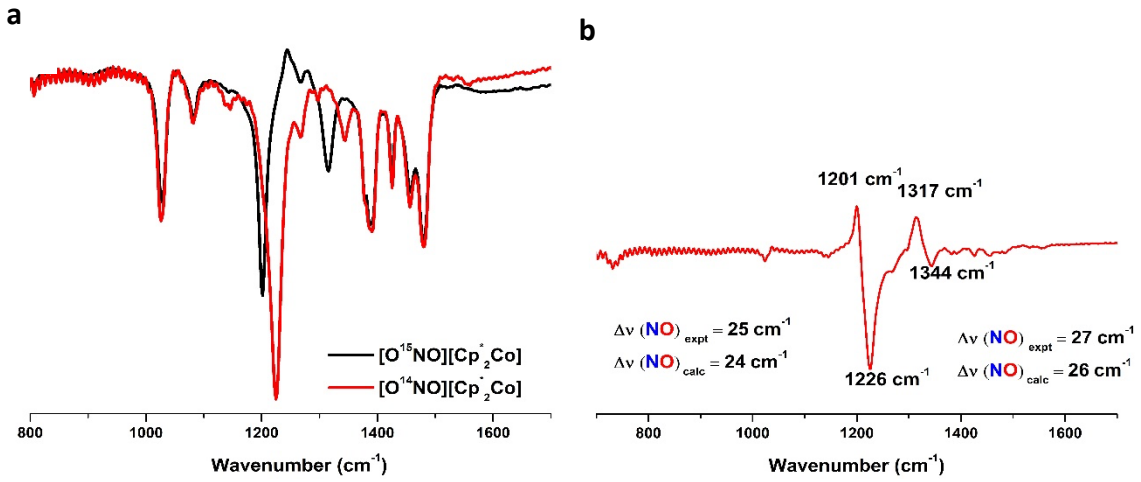

Figure 2. (a) FT-IR spectra of $[Cp^*_2Co][NO_2]$ (**1**) (red trace) and $[Cp^*_2Co][NO_2]$ (**1-^{15}N**) (black trace). (b) The difference spectrum between **1** (down) and **1-^{15}N** (up).

4. Synthesis and Characterization of $[Cp^*_2Co][(C_6F_5)_3B\text{-}ONO]$ (2)

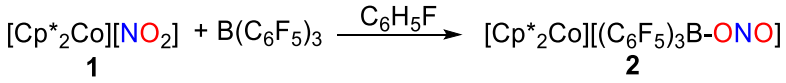

Scheme 2. Synthesis of $[Cp^*_2Co][(C_6F_5)_3B\text{-}ONO]$ (**2**)

$B(C_6F_5)_3$ (0.272 g, 0.532 mmol) in fluorobenzene was directly added to a solution of $[Cp^*_2Co][NO_2]$ (0.200 g, 0.532 mmol) in fluorobenzene (*ca.* 3 mL). The solution was shaken and the resultant yellow solution was filtered through Celite, layered with pentane and kept at -40 °C overnight to obtain X-ray quality crystals (0.370 g, 0.416 mmol) in 78% yield. **2-^{15}N** was prepared similarly from **1-^{15}N**.

^{1}H NMR (400 MHz, CD_2Cl_2): δ -1.69 (s, 30 H, CH_3) (Figure S3);

^{19}F NMR (376 MHz, CD_2Cl_2): δ -132.96, -160.92, -165.81 (Figure S4);

^{15}N NMR (41 MHz, CD_2Cl_2): δ 599.69 (**2-^{15}N**);

^{11}B NMR - (128 MHz, CD_2Cl_2): δ 0.95 (s, 1 B)

^{13}C{^{1}H} NMR (100 MHz, CD_2Cl_2): δ 148.50, 139.21, 136.49, 122.23, 94.56, 8.28;

FT-IR (cm^{-1}): 1561 ν(^{14}NO); 1531 ν(^{15}NO); Hooke's law predicts $^{15N/14N}\Delta\nu$ = 30 cm^{-1} (Figure S5). The IR spectra were taken as a thin film by evaporating a dichloromethane solution of **2** on a KBr window. Anal.Calcd for $C_{39}H_{32}BCl_2CoF_{15}NO_2$: C, 48.71; H, 3.47; N, 1.42. Found: C, 48.64; H, 3.20; N, 1.55

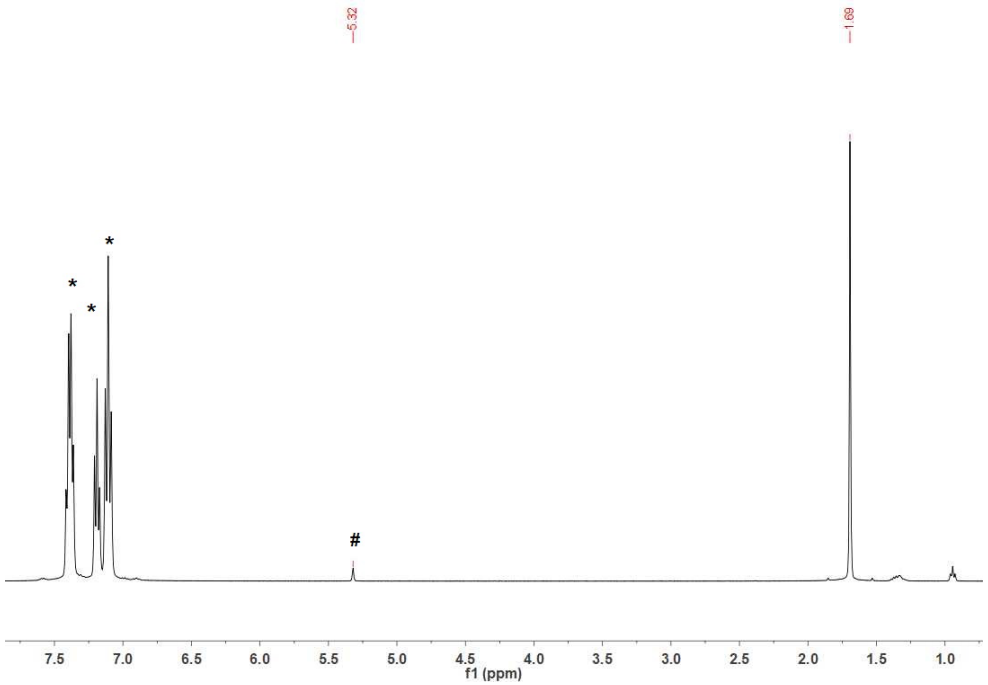

Figure 3. ^{1}H NMR spectrum (400 MHz, CD_2Cl_2) of $[Cp^*_2Co][(C_6F_5)_3B\text{-}ONO]$ (**2**). The resonances marked with (*) and (#) belong to solvent (C_6H_5F) and the residual proton impurities of CD_2Cl_2, respectively.

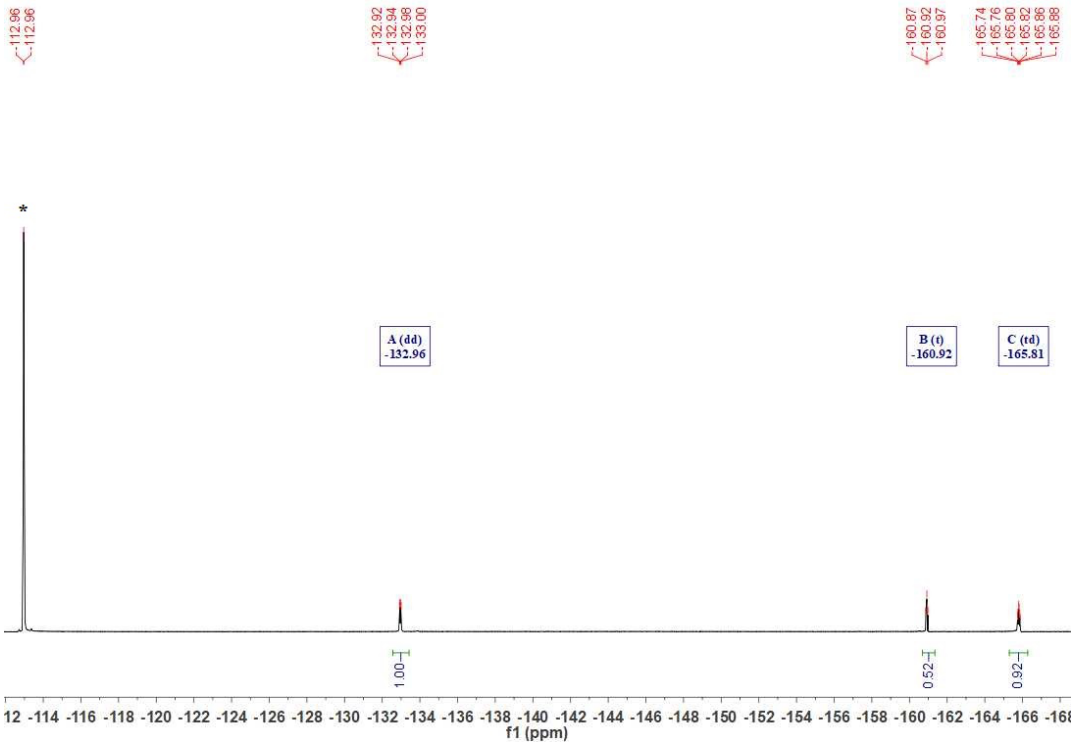

Figure 4. ^{19}F NMR spectrum (376 MHz, CD_2Cl_2) of $[Cp^*_2Co][(C_6F_5)_3B\text{-}ONO]$ (**2**). The resonance marked with (*) belong to solvent (C_6H_5F) residual peak used as an internal standard.

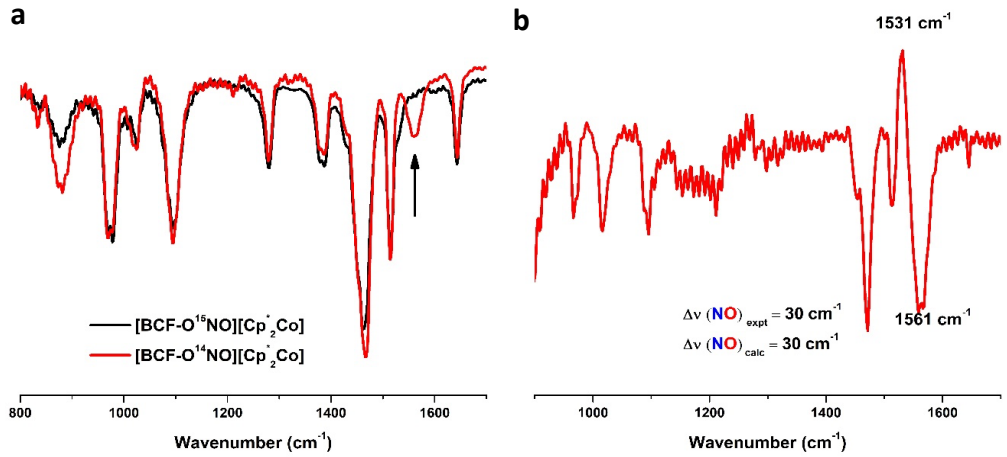

Figure 5. (a) FT-IR spectra of $[Cp^*_2Co][(C_6F_5)_3B\text{-}ONO]$ (**2**) (red trace) and $[Cp^*_2Co][(C_6F_5)_3B\text{-}O^{15}NO]$ (**2-^{15}N**) (black trace). (b) The difference spectrum between **2** (down) and **2-^{15}N** (up).

5. Synthesis and Characterization of $[Cp^*_2Co][(C_6F_5)_3B\text{-}ONO\text{-}B(C_6F_5)_3]$ (3)

$$\underset{\mathbf{1}}{[Cp^*_2Co][NO_2]} + 2\ B(C_6F_5)_3 \xrightarrow{C_6H_5F} \underset{\mathbf{3}}{[Cp^*_2Co][(C_6F_5)_3B\text{-}ONO\text{-}B(C_6F_5)_3]}$$

Scheme 3. Synthesis of $[Cp^*_2Co][(C_6F_5)_3B\text{-}ONO\text{-}B(C_6F_5)_3]$ (**3**)

$B(C_6F_5)_3$ (0.261 g, 0.509 mmol) in fluorobenzene was directly added to a solution of $[Cp^*_2Co][NO_2]$ (0.100 g, 0.532 mmol) in fluorobenzene (*ca.* 3 mL) at -40 °C. The solution was shaken, and the resultant yellow solution was filtered through Celite and pentane (*ca.* 6 mL) was added to initiate crystallization. The vial kept at -40 °C to obtain X-ray quality crystals (0.315 g, 0.416 mmol) in 72% yield. **3-^{15}N** was prepared similarly from **2-^{15}N**.

^{1}H NMR (400 MHz, CD_2Cl_2): δ 1.7 (s, 30 H, CH_3) (Figure S6);

^{19}F NMR (376 MHz, CD_2Cl_2): δ -132.19, -157.01, -164.42. (Figure S7);

^{15}N NMR (41 MHz, CD_2Cl_2): δ 615.67 (**3-^{15}N**);

^{11}B NMR - (128 MHz, CD_2Cl_2): δ 5.85 (s, 1 B)

$^{13}C\{^1H\}$ NMR (100 MHz, CD_2Cl_2): δ 148.42, 140.77, 137.41, 117.15, 94.96, 8.34;

FT-IR (cm^{-1}): 1265 ν(^{14}NO); 1240 ν(^{15}NO); Hooke's law predicts $^{15N/14N}\Delta\nu$ =24 cm^{-1}(Figure S8). The IR spectra were taken as a thin film by evaporating a dichloromethane

solution of **3** on a KBr window. Anal. Calcd for $C_{56}H_{30}B_2CoF_{30}NO_2$: C, 48.07; H, 2.16; N, 1.00. Found: C, 47.87; H, 2.37; N, 1.08

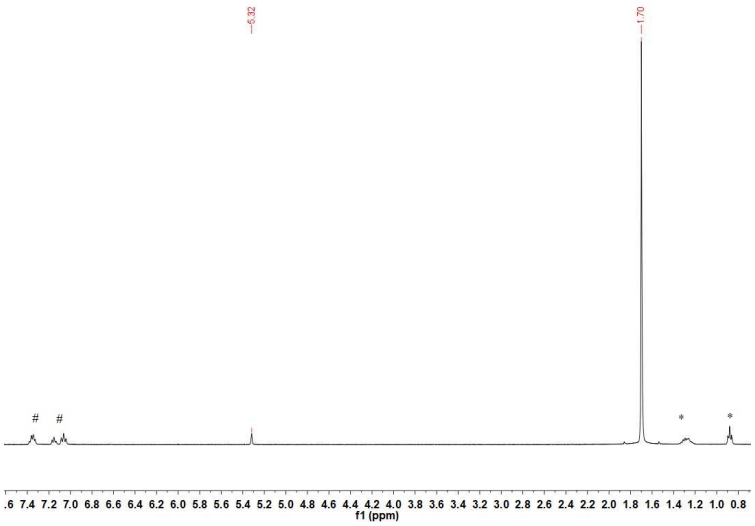

Figure 6. ^{1}H NMR spectrum (400 MHz, CD_2Cl_2) of $[Cp^*_2Co][(C_6F_5)_3B\text{-}ONO\text{-}B(C_6F_5)_3]$ (**3**). The resonances shown by # and * belong to solvent residual peak for C_6H_5F and pentane, respectively.

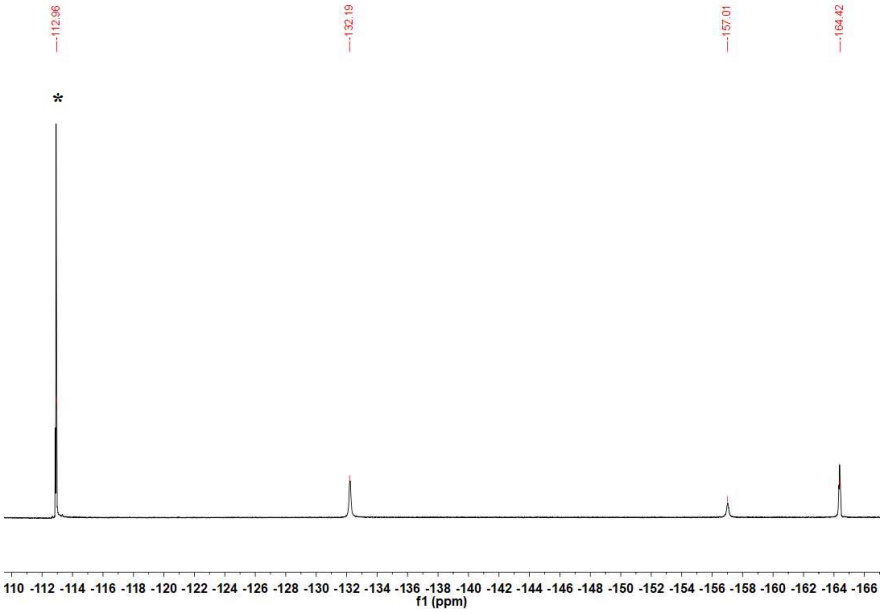

Figure 7. ^{19}F NMR spectrum (376 MHz, CD_2Cl_2) of $[Cp^*_2Co][(C_6F_5)_3B\text{-}ONO\text{-}B(C_6F_5)_3]$ (**3**). The resonance marked with (*) belongs to C_6H_5F that is used as an internal standard.

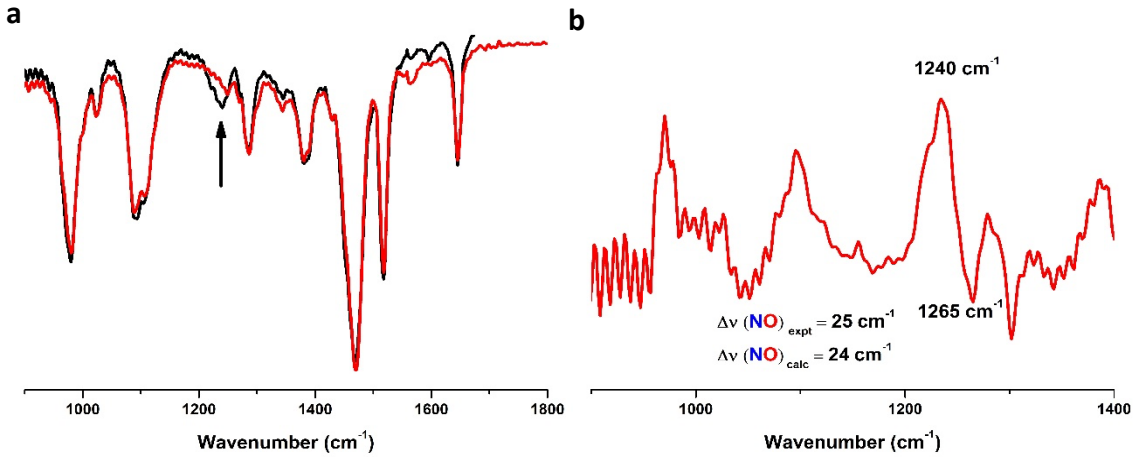

Figure 8. (a) FT-IR spectra of $[Cp^*_2Co][(C_6F_5)_3B\text{-}ONO\text{-}B(C_6F_5)_3]$ (**3**) (red trace) and $[Cp^*_2Co][(C_6F_5)_3B\text{-}O^{15}NO\text{-}B(C_6F_5)_3]$ (**3-^{15}N**) (black trace). (b) The difference spectrum between **3** (down) and **3-^{15}N** (up).

6. Synthesis and Characterization of $[Cp^*_2Co]_2[(C_6F_5)_3B\text{-}ONO\text{-}B(C_6F_5)_3]$ (4).

$$[Cp^*_2Co][(C_6F_5)_3B\text{-}ONO\text{-}B(C_6F_5)_3] \;(\mathbf{3}) + Cp^*_2Co \xrightarrow{C_6H_5F} [Cp^*_2Co]_2[(C_6F_5)_3B\text{-}ONO\text{-}B(C_6F_5)_3] \;(\mathbf{4})$$

Scheme 4. Synthesis of $[Cp^*_2Co]_2[(C_6F_5)_3B\text{-}ONO\text{-}B(C_6F_5)_3]$ (**4**)

Cp^*_2Co (0.074 g, 0.224 mmol) in fluorobenzene was dropwise added to a solution of $[Cp^*_2Co][(C_6F_5)_3B\text{-}ONO\text{-}B(C_6F_5)_3]$ (0.315 g, 0.224 mmol) in fluorobenzene (*ca.* 5 mL) at -40 °C. The solution was shaken, and the resultant gray solution was filtered through a filtering pad kept at -40 °C to obtain X-ray quality crystals (0.350 g, 0.182 mmol) in 90% yield. **4-^{15}N** was prepared similarly from **3-^{15}N**.

FT-IR (cm^{-1}): 1010 $\nu(^{14}NO)$; 990 $\nu(^{15}NO)$; Hooke's law predicts $^{15N/14N}\Delta\nu = 20$ cm^{-1} (Figure S9).The IR spectra were taken as a thin film by evaporating a dichloromethane solution of **4** on a KBr window.$C_{76}H_{30}B_2CoF_{30}NO_2$: C, 52.80; H, 3.50; N, 0.81. Found: C, 53.05; H, 3.64; N, 0.83.

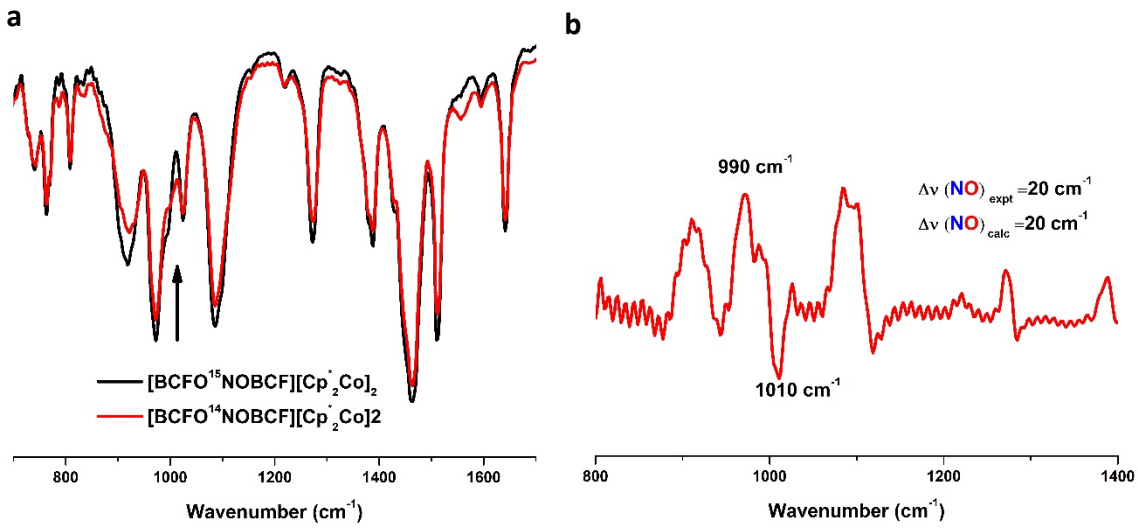

Figure 9. (a) FT-IR spectra of $[Cp^*_2Co]_2[(C_6F_5)_3B\text{-}ONO\text{-}B(C_6F_5)_3]$ (**4**) (red trace) and $[Cp^*_2Co]_2[(C_6F_5)_3B\text{-}O^{15}NO\text{-}B(C_6F_5)_3]$ (**4-^{15}N**) (black trace). (b) The difference spectrum between **4** (down) and **4-^{15}N** (up).

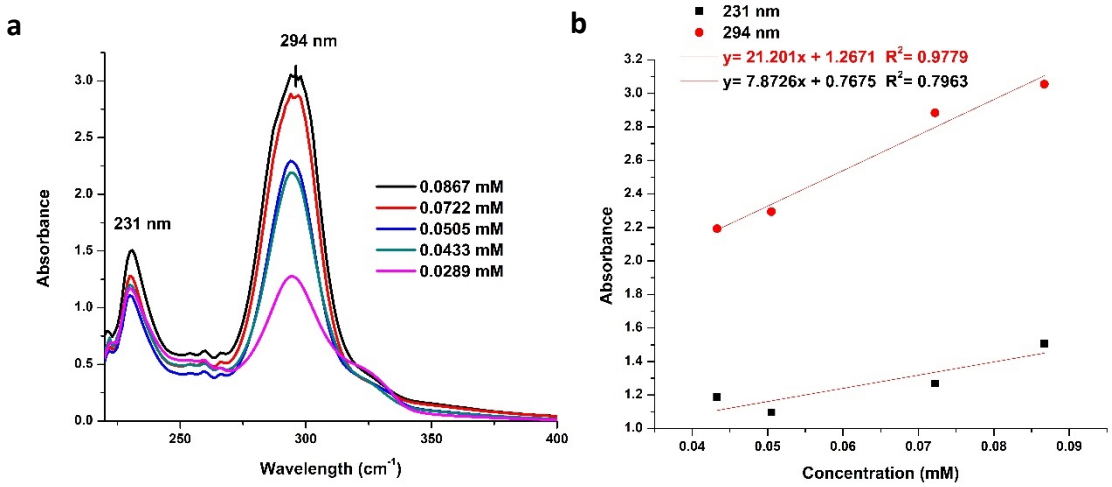

Figure 10. (a) UV-Vis spectra of $[Cp^*_2Co]_2[(C_6F_5)_3B\text{-}ONO\text{-}B(C_6F_5)_3]$ in dichloromethane at 25 °C at different concentrations. (b) Beer's law plot for **4** depicts λ_{max} = 294 nm (ε = 21000 $M^{-1}cm^{-1}$) and λ_{max} = 231 nm (ε = 7900 $M^{-1}cm^{-1}$)

Table 1. Summary of NO stretching frequencies observed in compounds **1**, **2**, **3** and **4**.

Compound	ν(NO) cm^{-1}
$[Cp^*_2Co][NO_2]$ (**1**)	1226, 1344
$[Cp^*_2Co][(C_6F_5)_3B\text{-}ONO]$ (**2**)	1561
$[Cp^*_2Co][(C_6F_5)_3B\text{-}ONO\text{-}B(C_6F_5)_3]$ (**3**)	1265
$[Cp^*_2Co]_2[(C_6F_5)_3B\text{-}ONO\text{-}B(C_6F_5)_3]$ (**4**)	1010

7. Reaction of $[Cp^*_2Co]_2[(C_6F_5)_3B\text{-}ONO\text{-}B(C_6F_5)_3]$ with CF_3COOH

$$[Cp^*_2Co]_2[(C_6F_5)_3B\text{-}ONO\text{-}B(C_6F_5)_3] \;(\mathbf{4}) + 2\ CF_3COOH \xrightarrow{C_6H_5F} [Cp^*_2Co][(C_6F_5)_3B\text{-}OC(O)CF_3] \;(\mathbf{5}) + H_2O + NO$$

To a solution of $[Cp^*_2Co]_2[(C_6F_5)_3B\text{-}ONO\text{-}B(C_6F_5)_3]$ (**4**) (0.03 g, 0.0173 mmol, 2 equiv.) in fluorobenzene was added CF_3COOH (0.034 mL, 1 M) in fluorobenzene. The color of the solution changed from light gray to light yellow with concomitant NO gas (64%) evolution (for NO gas trapping experiments see Section 9). After 30 min stirring the resultant solution was analyzed by ^1H NMR and ^{19}F NMR spectroscopy which confirms the formation of $[Cp^*_2Co][(C_6F_5)_3B\text{-}OC(O)CF_3]$ (**5**) in 85% yield.

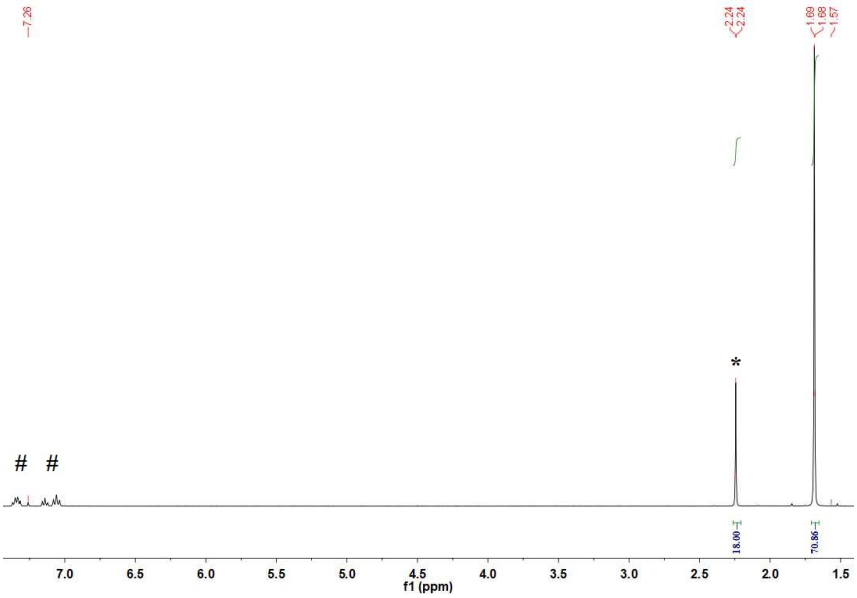

Figure 11. ^1H NMR spectrum (400 MHz, $CDCl_3$) for the reaction of $[Cp^*_2Co]_2[(C_6F_5)_3B\text{-}ONO\text{-}B(C_6F_5)_3]$ (**4**) with 2 equiv. $HO(O)CF_3$ to give $[Cp^*_2Co][(C_6F_5)_3B\text{-}OC(O)CF_3]$ (**5**). The resonances marked with (*) and (#) belong to hexamethylbenzene used as internal standard and solvent (C_6H_5F) residual peaks, respectively.

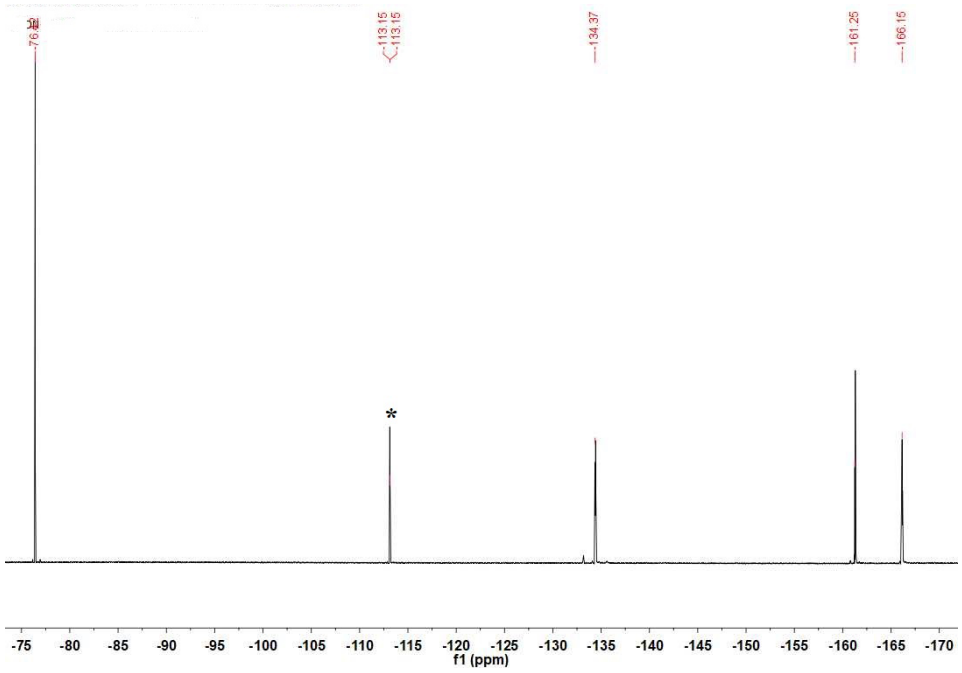

Figure 12. ^{19}F NMR spectrum (376 MHz**,** $CDCl_3$) for the reaction of $[Cp^*_2Co]_2[(C_6F_5)_3B\text{-}ONO\text{-}B(C_6F_5)_3]$ (**4**) with 2 equiv. $CF_3C(O)OH$ to give $[Cp^*_2Co][(C_6F_5)_3B\text{-}OC(O)CF_3]$ (**5**). The resonance marked with (*****) belongs to solvent (C_6H_5F) residual peaks used as internal standard.

Isolation of $[Cp^*_2Co][(C_6F_5)_3B\text{-}OC(O)CF_3]$ (5)

To a solution of $[Cp^*_2Co]_2[(C_6F_5)_3B\text{-}ONO\text{-}B(C_6F_5)_3]$ (**4**) (0.1 g, 0.0578 mmol) in fluorobenzene was added CF_3COOH (0.113 mL, 1M, 0.115 mmol, 2 equiv.) in fluorobenzene. The color of the solution changed from gray to light yellow. The solution stirred for 30 min at RT, then the solvent was evaporated under vacuum to afford a yellow powder (0.040 g, 0.0419 mmol, 72%). X-ray quality crystals for $[Cp^*_2Co][B(C_6F_5)_3OC(O)CF_3]$ (**5**) were grown at -40 °C by layering a C_6H_5F solution with pentane.

^1H NMR (400 MHz, $CDCl_3$): δ 1.69 (s, 30 H, CH_3);

^{19}F NMR (376 MHz, $CDCl_3$): -76.47, -134.50, -161.42, -166.18;

^{11}B NMR (128 MHz, CD_2Cl_2): δ -3.80

$^{13}C\{^1H\}$ NMR (400 MHz, $CDCl_3$): δ 157.88, 147.96, 139.02, 135.36, 120.77, 94.14, 7.75.

Anal. Calcd for $C_{40}H_{30}BCoF_{18}O_2$: C, 50.34; H, 3.17; Found: C, 50.35; H, 3.12.

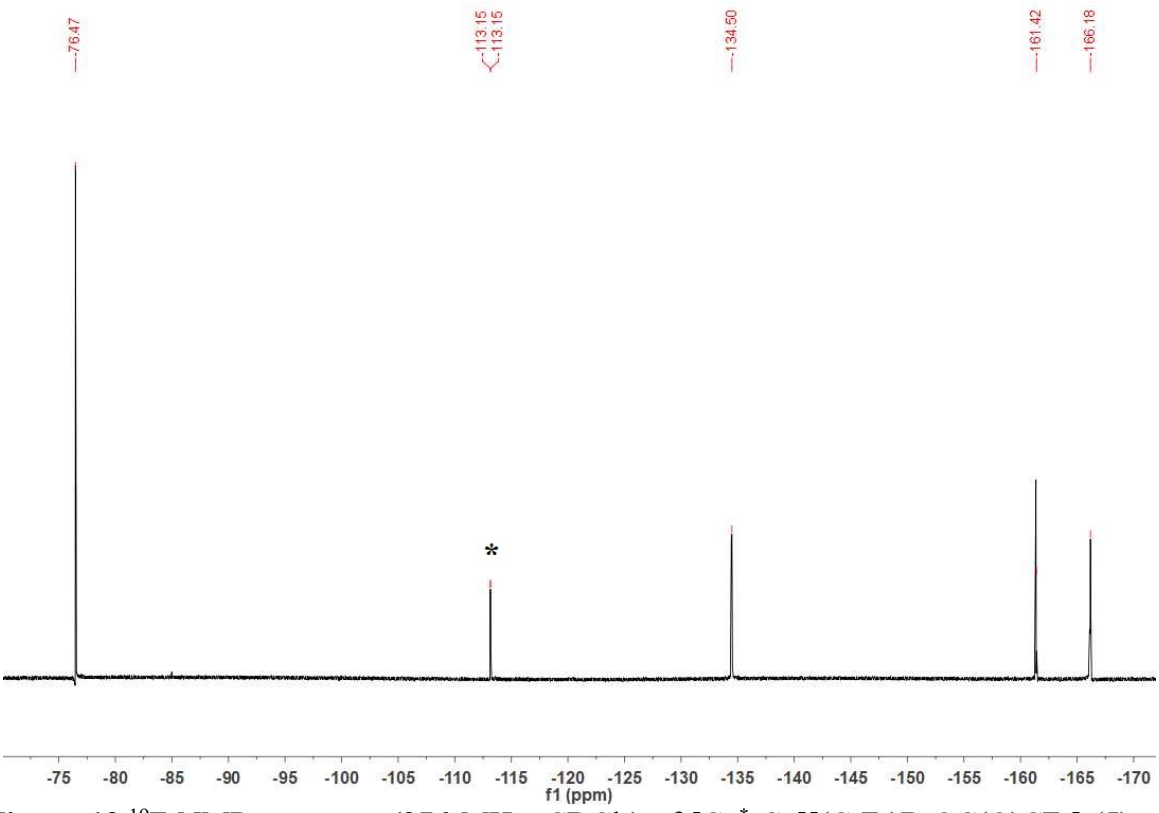

Figure 13. ^{19}F NMR spectrum (376 MHz, $CDCl_3$) of $[Cp^*_2Co][(C_6F_5)B\text{-}OC(O)CF_3]$ (**5**). The resonance marked with (*) belongs to the solvent residual peak for C_6H_5F (*) which also used as internal standard.

8. Reaction of $[Cp^*_2Co]_2[(C_6F_5)_3B\text{-}ONO\text{-}B(C_6F_5)_3]$ (4) with HBF_4

$$\underset{\mathbf{4}}{[Cp^*_2Co]_2[(C_6F_5)_3B\text{-}ONO\text{-}B(C_6F_5)_3]} + 2\ HBF_4 \xrightarrow{C_6H_5F} \underset{\mathbf{6}}{[Cp^*_2Co][(C_6F_5)_3B\text{-}F]} + H_2O + NO$$

To a solution of $[Cp^*_2Co]_2[(C_6F_5)_3B\text{-}ONO\text{-}B(C_6F_5)_3]$ (**4**) (0.02 g, 0.011 mmol) in fluorobenzene was added HBF_4 (0.023 mL, 0.5 M, 2 equiv.) in fluorobenzene. The color of the solution changed from light gray to light yellow with concomitant NO gas (62%) evolution (for NO gas trapping experiments see Section 9). After 30 min stirring the resultant solution was analyzed by ^{19}F NMR which confirms the formation of $[Cp^*_2Co][(C_6F_5)_3B\text{-}F]$ (**6**) in 78% yield.

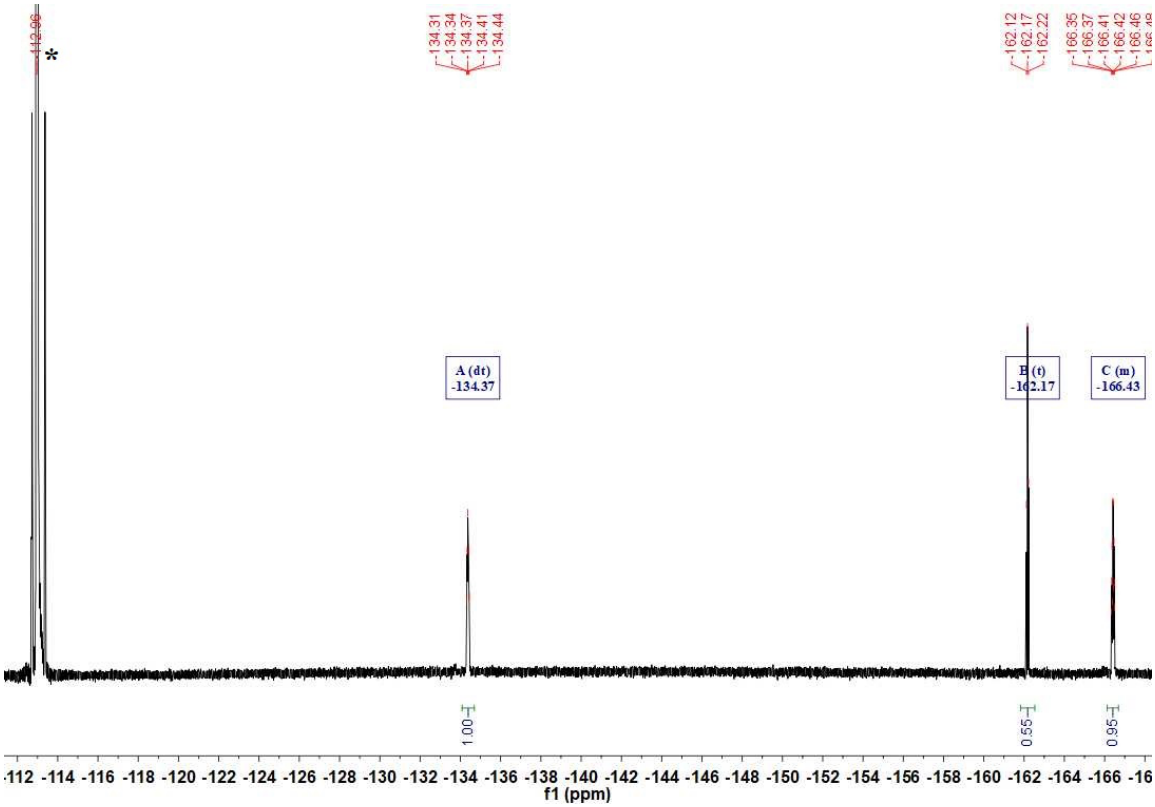

Figure 14. ^{19}F NMR spectrum (376 MHz, CD_2Cl_2) for the reaction of $[Cp^*_2Co]_2[(C_6F_5)_3B\text{-}ONO\text{-}B(C_6F_5)_3]$ (**4**) with 2 equiv. HBF_4. The resonance marked with (*) belongs to the solvent residual peak for C_6H_5F which also used as internal standard.

Isolation of $[Cp^*_2Co][(C_6F_5)_3B\text{-}F]$ (6)

To a solution of $[Cp^*_2Co]_2[(C_6F_5)_3B\text{-}ONO\text{-}B(C_6F_5)_3]$ (**4**) (0.1 g, 0.0578 mmol) in fluorobenzene was added HBF_4 (0.231 mL, 0.5 M, 0.231 mmol, 2 equiv.) in fluorobenzene. The color of the solution changed from gray to light yellow. The solution was shaken several times at room temperature then the solvent was evaporated under vacuum to afford a yellow powder (0.065 g, 0.075 mmol, 65%). X-ray quality crystals of $[Cp^*_2Co][(C_6F_5)_3B\text{-}F]$ (**6**) were grown at -40 °C by layering a C_6H_5F solution with pentane.

^1H NMR (400 MHz, $CDCl_3$): δ 1.69 (s, 30 H, CH_3);

^{19}F NMR (376 MHz, $CDCl_3$):, -134.89, -162.12, -166.47;

^{11}B NMR - (128 MHz, CD_2Cl_2): δ -1.08 (d, 1 B);

$^{13}C\{^1H\}$ NMR (400 MHz, $CDCl_3$): δ 148.88, 139.59, 137.34, 125.54, 94.96, 8.65. Anal. Calcd for $C_{38}H_{30}BCoF_{16}$: C, 53.05; H, 3.51; Found: C, 53.03; H, 3.58.

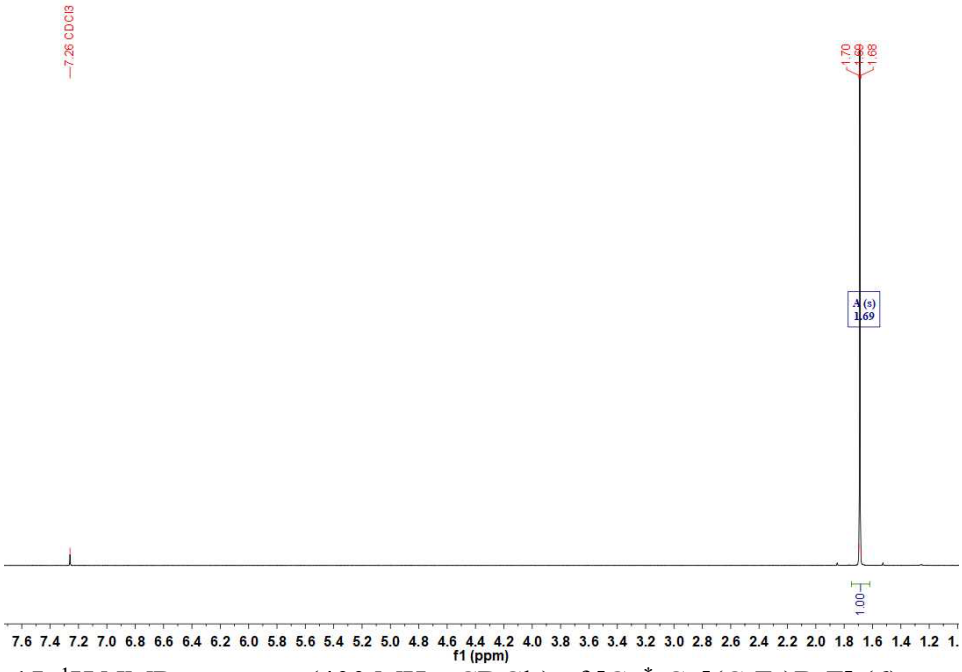

Figure 15. ^{1}H NMR spectrum (400 MHz, $CDCl_3$) of $[Cp^*_2Co](C_6F_5)B\text{-}F]$ (**6**).

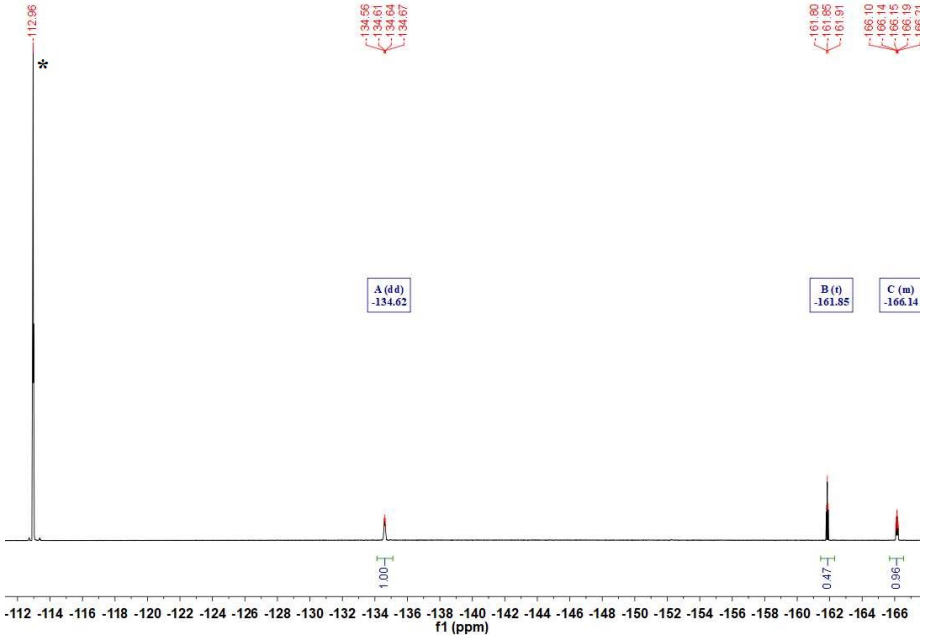

Figure S16. ^{19}F NMR spectrum (376 MHz**,** $CDCl_3$) of $[Cp^*_2Co][(C_6F_5)B\text{-}F]$ (**6**). The resonances marked with belong to the solvent residual peak for C_6H_5F which also used as internal standard.

9. Quantitative NO Trapping by (T(O-Me)PP)Co^{II} Complex

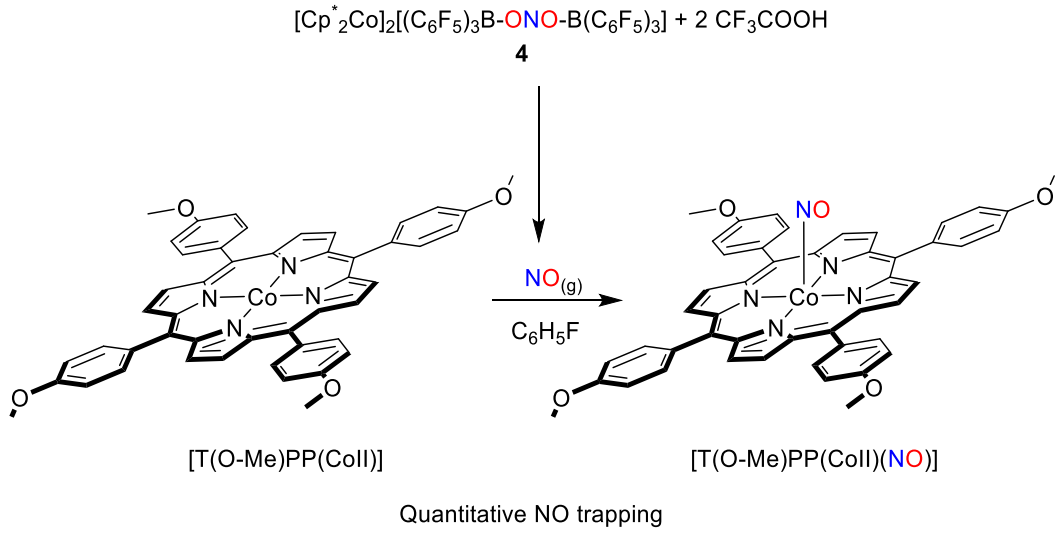

Scheme 5. Stoichiometric conversion of (T(O-Me)PP)Co^{II} to (T(O-Me)PP)CoNO utilized for NO quantification.

Quantitative trapping of nitric oxide was done using 5,10,15,20-Tetrakis(4-methoxyphenyl)-21*H*,23*H*-porphine cobalt(II) [T(O-Me)PP]Co^{II} complex. Commercially purchased [T(O-Me)PP]Co^{II} was purified by column chromatography to yield a pure purple powder before use. Quantification was based on the integration of the ^{1}H NMR spectrum of the [T(O-Me)PP]Co^{II}(NO) during each reaction in presence of a quantitative NMR (Q-NMR) standard. Here, we used hexamethylbenzene as the Q-NMR standard. [T(O-Me)PP]Co^{II} and [T(O-Me)PP]Co^{II}(NO) have completely different NMR profiles as shown in Figure S3 which makes them suitable for this analysis (resonance at δ 5.31 for [T(O-Me)PP]Co^{II} shifts to δ 4.07 for [T(O-Me)PP]Co^{II}(NO).

(T(O-Me)PP)Co^{II} complex (0.009 g, 0.011 mmol) dissolved in C_6H_5F in a small vial and placed in a larger vial. The larger vial was sealed with a septum. [Cp*$_2$Co]$_2$[(C$_6$F$_5$)$_3$B-ONO-B(C$_6$F$_5$)$_3$] (**4**) (0.02 g, 0.011 mmol) in fluorobenzene was injected to the big vial. Then a solution of CF_3COOH (0.092 mL, 0.25 M, 2 eq.) in fluorobenzene was injected to the inner vial and the solutions in both vials stirred for 2 hr. 0.5 mL of the cobalt (II) solution was transferred to an NMR tube for analysis.

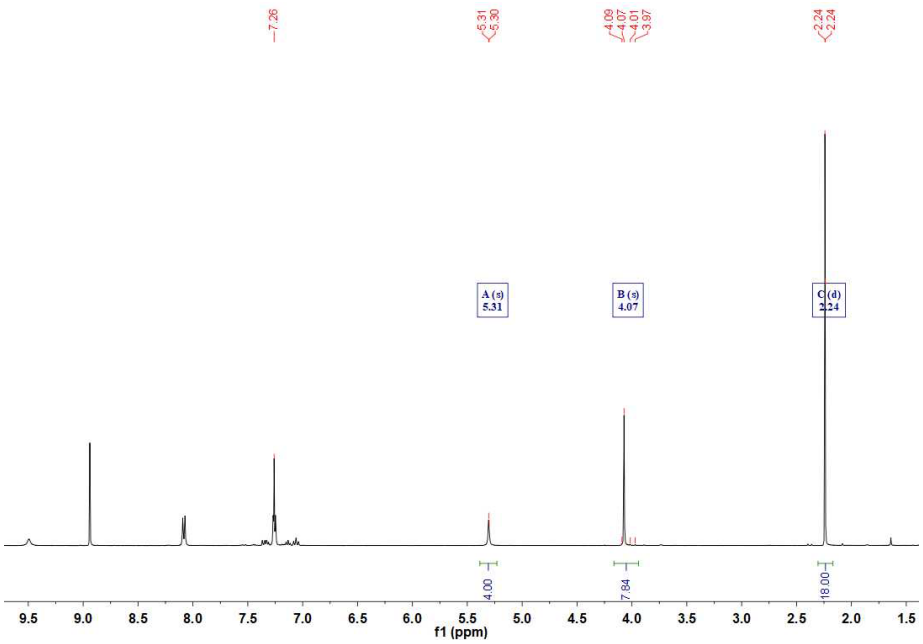

Figure 17. ^{1}H NMR spectrum (400 MHz, $CDCl_3$) of [T(O-Me)PP]Co^{II}(NO) generated from the reaction of $[Cp^*_2Co][(C_6F_5)_3B\text{-}ONO\text{-}B(C_6F_5)_3]$ (**4**) with 2 eq. CF_3COOH. The resonance at δ 5.31 for [T(O-Me)PP]Co^{II} shifts to δ 4.07 for [T(O-Me)PP]Co^{II}(NO). The resonance at δ 2.24 is for hexamethylbenzene used as internal standard.

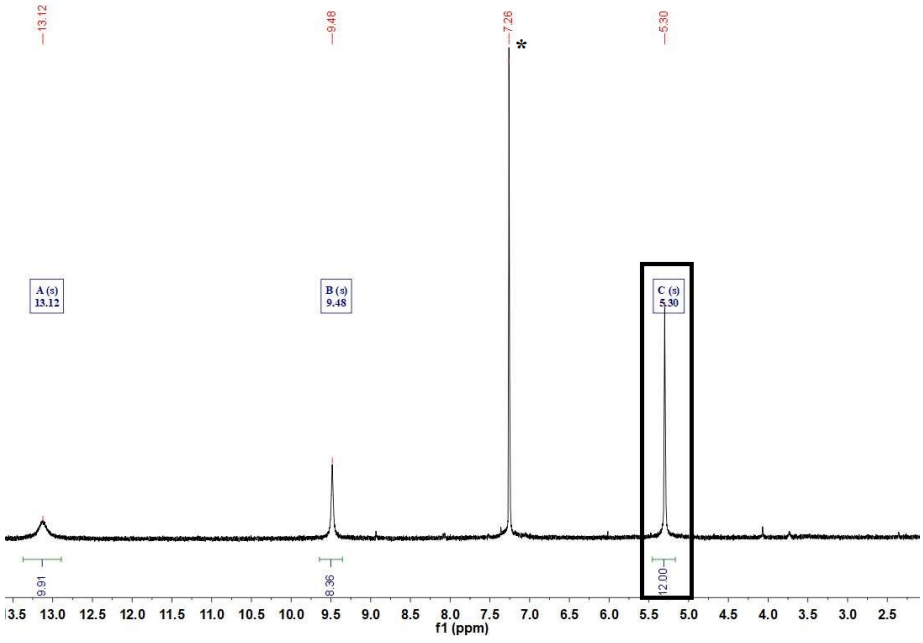

Figure 18. ^{1}H NMR spectrum (400 MHz, $CDCl_3$) of [T(O-Me)PP]Co^{II} The resonances marked with (*) belong to the residual proton impurities of CD_2Cl_2.

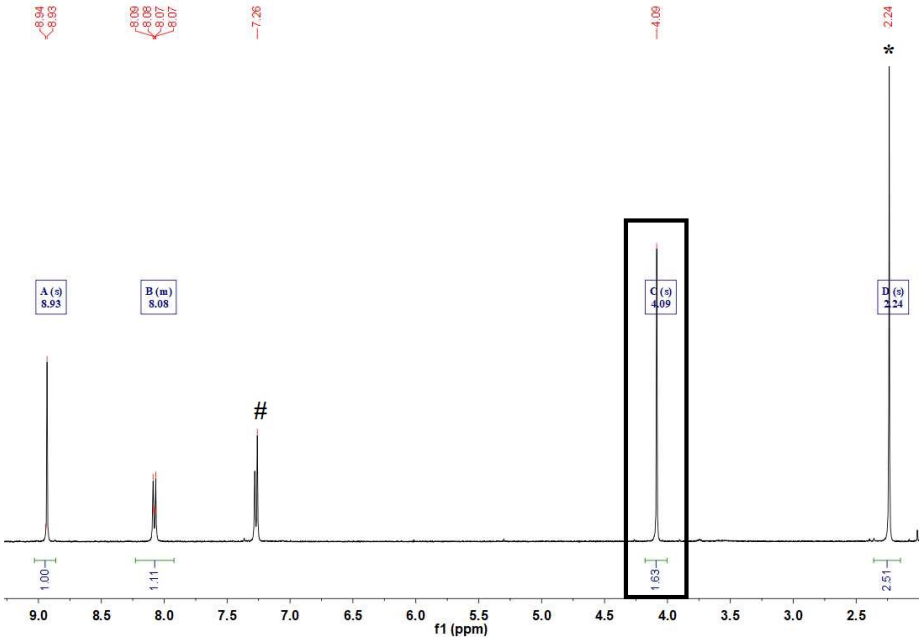

Figure 19. ^{1}H NMR spectrum (400 MHz, $CDCl_3$) of [T(O-Me)PP]Co^{II}(NO). The resonances marked with (*) and (#) belong to hexamethylbenzene used as internal standard and the residual proton impurities of CD_2Cl_2, respectively.

10. Triggering NO release from [Cp*$_2$Co]$_2$[BCF-ONO-BCF] via heat

$$[Cp^*_2Co]_2[(C_6F_5)_3B\text{-}ONO\text{-}B(C_6F_5)_3] \xrightarrow[\text{Heat}]{C_6H_5F} NO$$

4

A solution of [Cp*$_2$Co]$_2$[$(C_6F_5)_3$B-ONO-B$(C_6F_5)_3$] (**4**) (0.030 g, 0.0173 mmol) dissolved in fluorobenzene was placed in a vial and heated at 75 °C for 48 h. The color of the solution changed from light orange to light yellow with concomitant NO gas (65%) evolution (for NO gas trapping experiments see Section 9). X-ray crystallography confirms the formation of [(η^5-$C_5Me_4CH_2$-B$(C_6F_5)_3$)CoCp*] (**7**) as one of the products for this reaction. Further attempts to identify other decay products were not successful.

11. Reaction of $[Cp^*_2Co]_2[(C_6F_5)_3B\text{-}ONO\text{-}B(C_6F_5)_3]$ with NO

$$[Cp^*_2Co]_2[(C_6F_5)_3B\text{-}ONO\text{-}B(C_6F_5)_3] \ (\mathbf{4}) + 3\ NO \xrightarrow{C_6H_5F} 2\ [Cp^*_2Co][(C_6F_5)_3B\text{-}ONO] \ (\mathbf{2}) + N_2O$$

To a solution of $[Cp^*_2Co]_2[(C_6F_5)_3B\text{-}ONO\text{-}B(C_6F_5)_3]$ (**4**) (0.03 g, 0.017 mmol) in fluorobenzene was added NO (3 eq., 0.052 mmol, 1.16 mL, 1.0 atm) in fluorobenzene. The color of the solution changed from light gray to light yellow in a course of 30 min with concomitant N_2O gas (43%) evolution (N_2O gas was quantified by GC). After 30 min stirring the resultant solution was analyzed by ^{19}F NMR which confirms the formation of $[Cp^*_2Co][(C_6F_5)_3B\text{-}ONO]$ (**2**) in 92% yield.

Quantification of N_2O. The Warren lab routinely uses this general technique that employs gas chromatography for the quantification of N_2O gas produced in chemical reactions that involves the generation of a calibration curve.[3] Gas chromatography was performed on a Gow-Mac GC (Model 69-400 TCD) equipped with a TCD as well as a 6' × 1/8" Molesieve 13x column. The carrier gas was He, and throughout the entire separation, the column was kept at 60 °C, while the detector was at 100 °C. Using identical reaction vessels and solvent amounts, the identification and quantification of N_2O was accomplished by withdrawing 250 µL of the headspace using a 250 µL Hamilton 1725 sample lock gastight syringe equipped with a large removable needle (22s ga, 2 in, point style 2).

A calibration curve was generated by preparing vials containing known amounts of pure N_2O gas for reference. This was accomplished by injecting varying amounts of N_2O in a stirring solution of C_6H_5F (3 mL) contained in 20 mL glass-vials, capped with rubber septum and sealed with parafilm. Quantification of N_2O was accomplished by withdrawing 250 µL of the headspace using a gastight syringe and injecting into the GC. The calibration curve was generated by plotting the area of N_2O (as obtained from the gas chromatograms) vs. mL of N_2O added. As this is a general method, the same data for the calibration curve (Figure 20) appear in the supporting information of a recent publication from the Warren lab.[4]

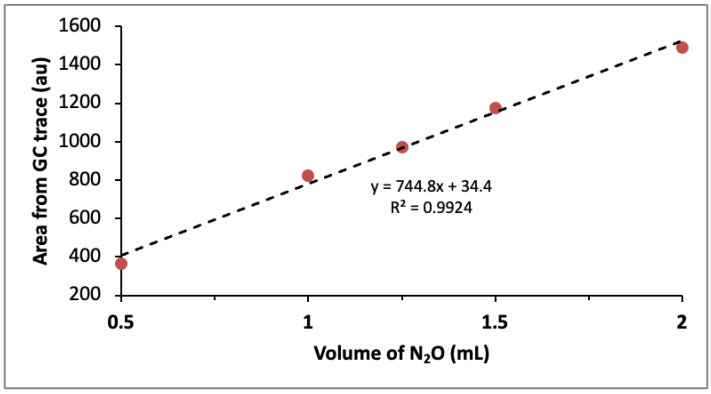

N2O injected (mL)	GC Area
0.5	366
1	823
1.25	973
1.5	1175
2	1490

Figure 20. Calibration curve used for the quantification of N_2O.

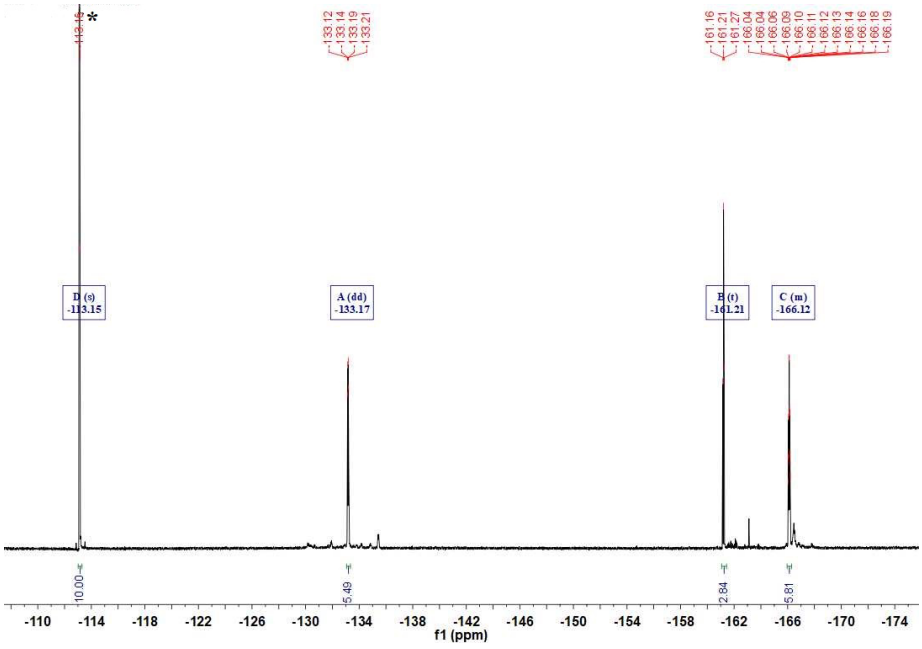

Figure S21. ^{19}F NMR spectrum (376 MHz**,** $CDCl_3$) for the reaction of $[Cp^*_2Co][(C_6F_5)_3B\text{-}ONO\text{-}B(C_6F_5)_3]$ (**4**) with 3 equiv. NO gas. The resonances marked with (*) solvent (C_6H_5F) residual peaks also used as internal standard.

12. Mechanistic studies for the reaction of $[Cp^*_2Co]_2[(C_6F_5)_3B\text{-}ONO\text{-}B(C_6F_5)_3]$ with NO: Isotopic Labeling

Reaction of $[Cp^*_2Co]_2[(C_6F_5)_3B\text{-}O^{14}NO\text{-}B(C_6F_5)_3]$ with ^{15}NO: quantification of $[Cp^*_2Co][(C_6F_5)_3B\text{-}O^{15}NO]$ by ^{15}N NMR

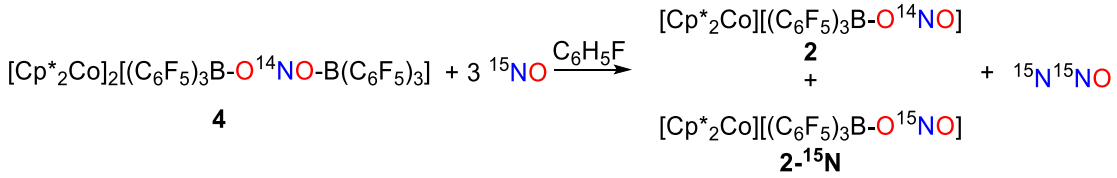

4

To a solution of $[Cp^*_2Co]_2[(C_6F_5)_3B\text{-}O^{14}NO\text{-}B(C_6F_5)_3]$ (**4**) (0.05 g, 0.028 mmol) in fluorobenzene was added ^{15}NO (3 equiv., 0.086 mmol, 1.94 mL, 1.0 atm) in fluorobenzene. The color of the solution changed from light gray to light yellow over the course of 30 min. After 30 min stirring the resultant solution was analyzed by ^{15}N NMR which confirms the formation of $[Cp^*_2Co][(C_6F_5)_3B\text{-}O^{15}NO]$ (**2-^{15}N**) in 50% yield.

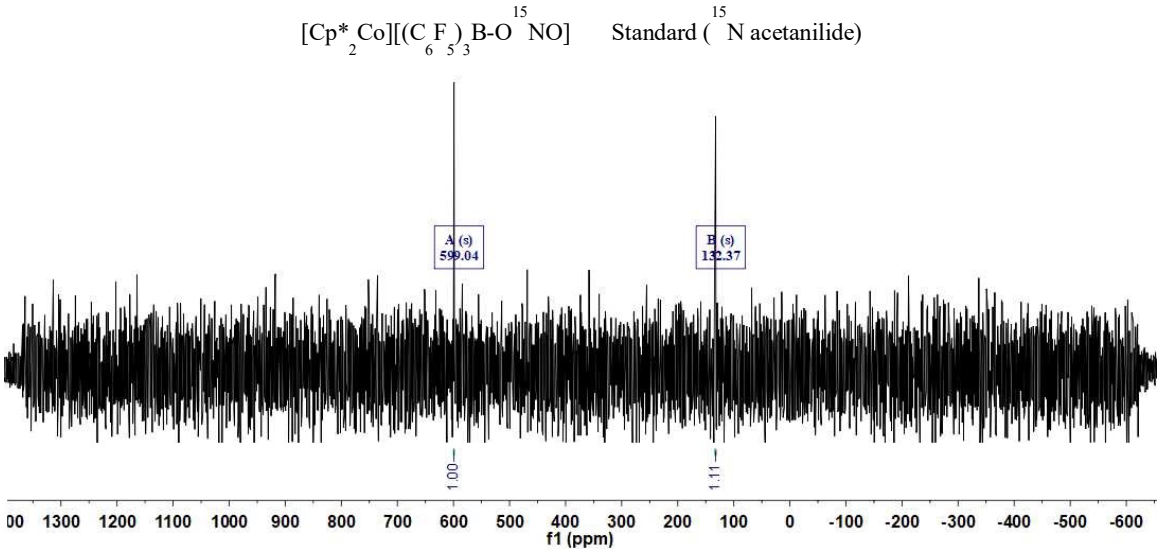

Figure 22. ^{15}N NMR spectrum (41 MHz, CD_2Cl_2) for the reaction of $[Cp^*_2Co]_2[(C_6F_5)_3B\text{-}ONO\text{-}B(C_6F_5)_3]$ (**4**) with 3 equiv. ^{15}NO gas.

Reaction of $[Cp^*_2Co]_2[(C_6F_5)_3B\text{-}O^{14}NO\text{-}B(C_6F_5)_3]$ with ^{15}NO: IR detection of $^{15}N^{15}NO$

To a solution of $[Cp^*_2Co]_2[(C_6F_5)_3B\text{-}O^{14}NO\text{-}B(C_6F_5)_3]$ (**4**) (0.05 g, 0.028 mmol) in fluorobenzene was added ^{15}NO (3 equiv., 0.086 mmol, 1.94 mL, 1.0 atm) in fluorobenzene. The color of the solution changed from light gray to light yellow over the course of 30 min. After 30 min stirring the resultant solution was analyzed by solution IR which confirms the formation of $^{15}N^{15}NO$. The solution IR stretching frequency for $^{15}N^{15}NO$ (2152 cm^{-1}) is in agreement with previously reported values.[5,6]

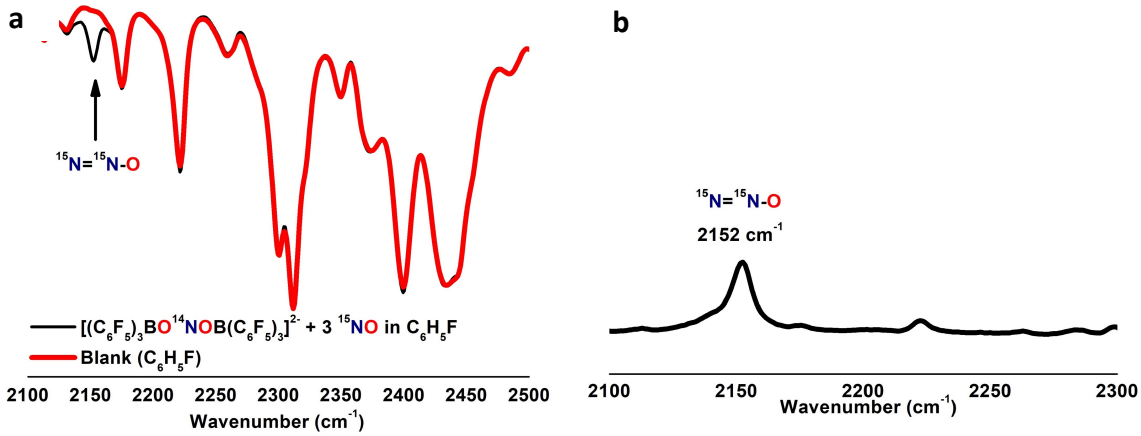

Figure 23. (a) IR spectrum (solution IR, C_6H_5F) for the reaction of $[Cp^*_2Co]_2[(C_6F_5)_3B\text{-}ONO\text{-}B(C_6F_5)_3]$ (**4**) with 3 equiv. ^{15}NO gas. (b) The difference spectrum between IR spectrum of the reaction mixture and blank C_6H_5F.

Reaction of $[Cp^*_2Co]_2[(C_6F_5)_3B\text{-}O^{15}NO\text{-}B(C_6F_5)_3]$ with ^{14}NO: quantification of $[Cp^*_2Co][(C_6F_5)_3B\text{-}O^{15}NO]$ by ^{15}N NMR

$$[Cp^*_2Co]_2[(C_6F_5)_3B\text{-}O^{15}NO\text{-}B(C_6F_5)_3] \text{ (4-}^{15}\text{N)} + 3\ ^{14}NO \xrightarrow{C_6H_5F} [Cp^*_2Co][(C_6F_5)_3B\text{-}O^{14}NO] \text{ (2)} + [Cp^*_2Co][(C_6F_5)_3B\text{-}O^{15}NO] \text{ (2-}^{15}\text{N)} + {}^{14}N^{14}NO$$

To a solution of $[Cp^*_2Co]_2[(C_6F_5)_3B\text{-}O^{15}NO\text{-}B(C_6F_5)_3]$ (**4**) (0.05 g, 0.028 mmol) in fluorobenzene was added ^{14}NO (3 equiv., 0.086 mmol, 1.94 mL, 1.0 atm) in fluorobenzene. The color of the solution changed from light gray to light yellow over the course of 30 min. After 30 min stirring the resultant solution was analyzed by ^{15}N NMR which confirms the formation of $[Cp^*_2Co][(C_6F_5)_3B\text{-}O^{15}NO]$ (**2**) in 100% yield.

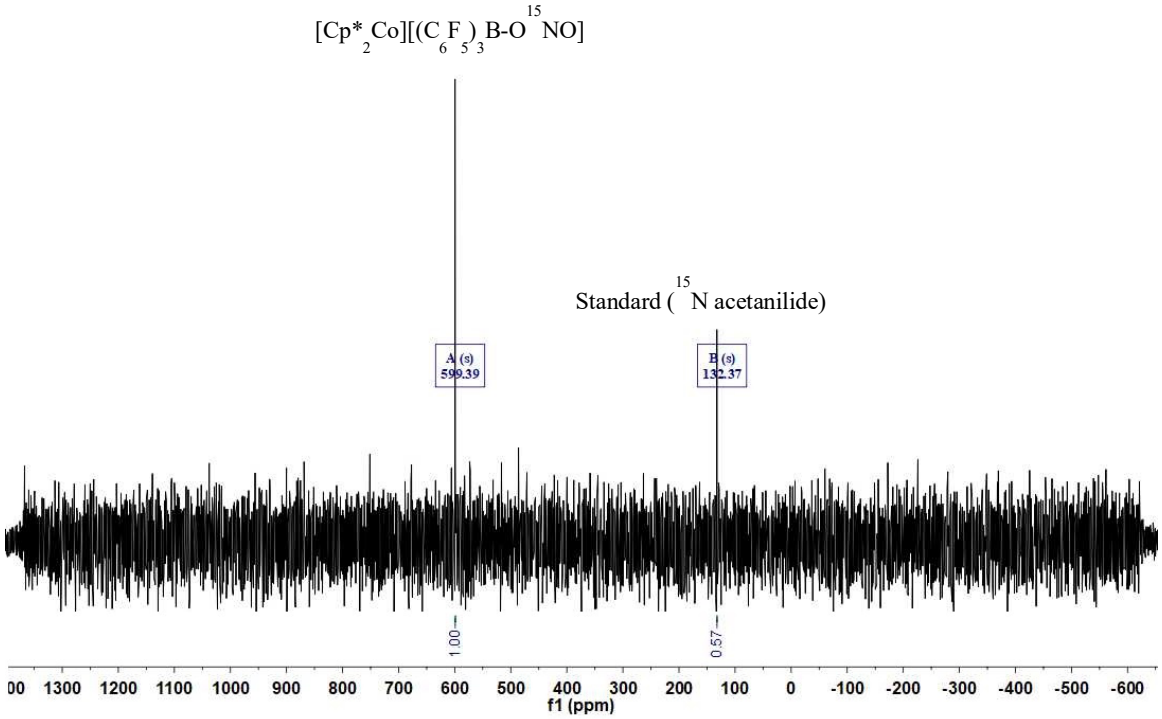

Figure 24. ^{15}N NMR spectrum (41 MHz**,** CD_2Cl_2) for the reaction of $[Cp^*_2Co]_2[(C_6F_5)_3B\text{-}O^{15}NO\text{-}B(C_6F_5)_3]$ (**4-^{15}N**) with 3 equiv. ^{14}NO gas.

Reaction of $[Cp^*_2Co]_2[(C_6F_5)_3B\text{-}O^{15}NO\text{-}B(C_6F_5)_3]$ with ^{14}NO: IR detection of $^{14}N^{14}NO$

To a solution of $[Cp^*_2Co]_2[(C_6F_5)_3B\text{-}O^{15}NO\text{-}B(C_6F_5)_3]$ (**4**) (0.05 g, 0.028 mmol) in fluorobenzene was added ^{14}NO (3 eq., 0.086 mmol, 1.94 mL, 1.0 atm) in fluorobenzene. The color of the solution changed from light gray to light yellow over the course of 30 min. After 30 min stirring the resultant solution was analyzed by solution IR which confirms the formation of $^{14}N^{14}NO$. The solution IR stretching frequency for $^{14}N^{14}NO$ (2152 cm^{-1}) is in agreement with previously reported values.[5,6]

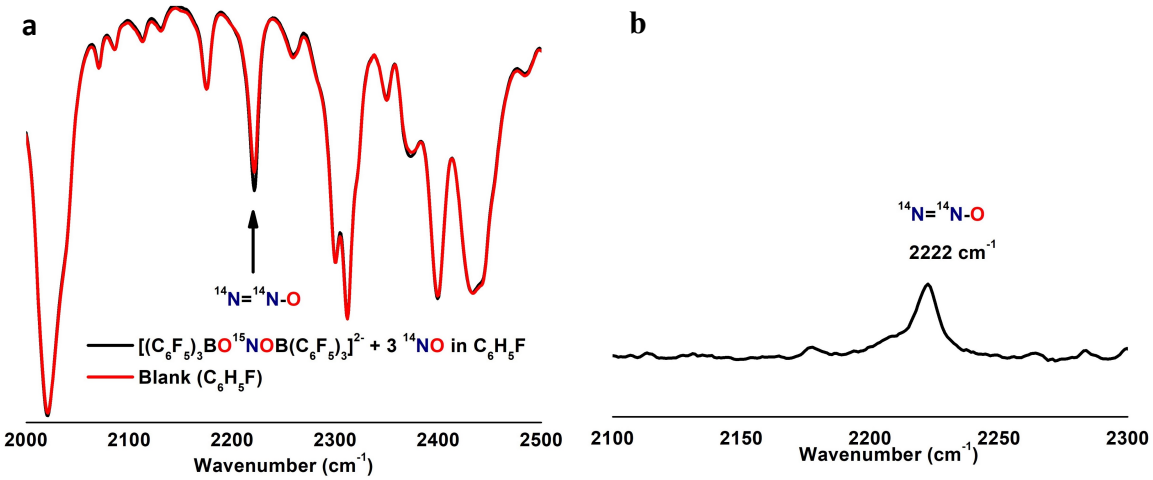

Figure 25. (a) IR spectrum (solution IR, C_6H_5F) for the reaction of $[Cp^*_2Co]_2[(C_6F_5)_3B\text{-}O^{15}NO\text{-}B(C_6F_5)_3]$ (**4-^{15}N**) with 3 equiv. ^{14}NO gas. (b) The difference spectrum between IR spectrum of the reaction mixture and blank C_6H_5F.

13. Cyclic Voltammetry Measurements

General Consideration. Cyclic voltammetry measurements were done at room temperature under dry nitrogen atmosphere of a glove box using BASi Epsilon Electrochemistry setup with three electrodes (working electrode: glassy carbon disk (0.071 cm^2), auxiliary electrode: platinum wire, reference electrode: $Ag/AgNO_3$). The reference electrode consisted of a Vycor-tipped glass tube having an Ag wire dipped in 1 mM $AgNO_3$ in CH_3CN. Ferrocene was added as an internal reference after each measurement. Thus, potentials were first measured with respect to $Fc^{+/0}$ couple and converted to NHE by adding 0.71 V.[6] The non-coordinating electrolyte bis(triphenylphosphine)iminiumtetrakis[3,5-bis(trifluoromethyl)phenyl]borate ([PPN][BAr^F_4]) was used for all cyclic voltammetry measurements.

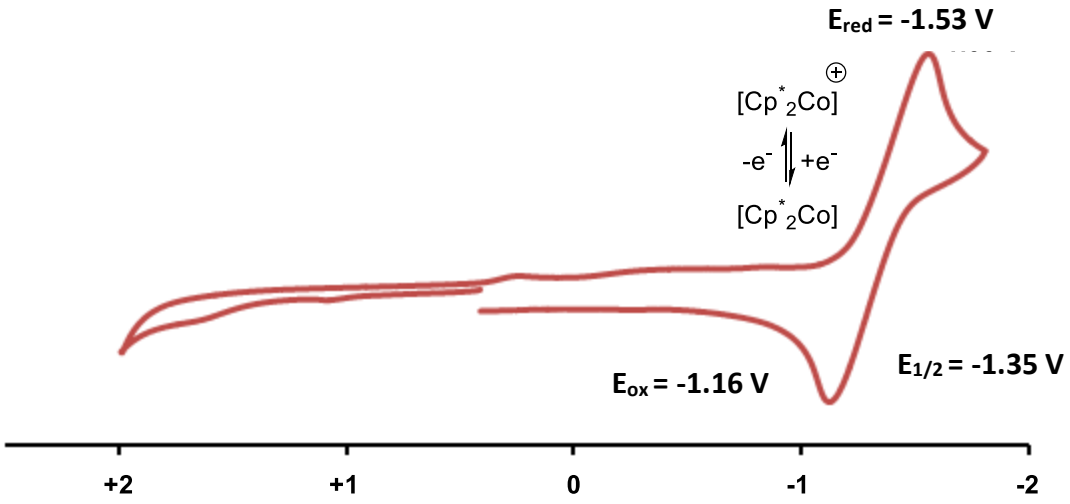

Figure 26. Cyclic voltammetry of $[Cp^*_2Co][(C_6F_5)_3B\text{-}ONO]$ (**2**) in fluorobenzene (4 mM) at 25 °C in presence of $[PPN][BAr^F_4]$ (0.1 M) with a scan rate of 100 mV/s.

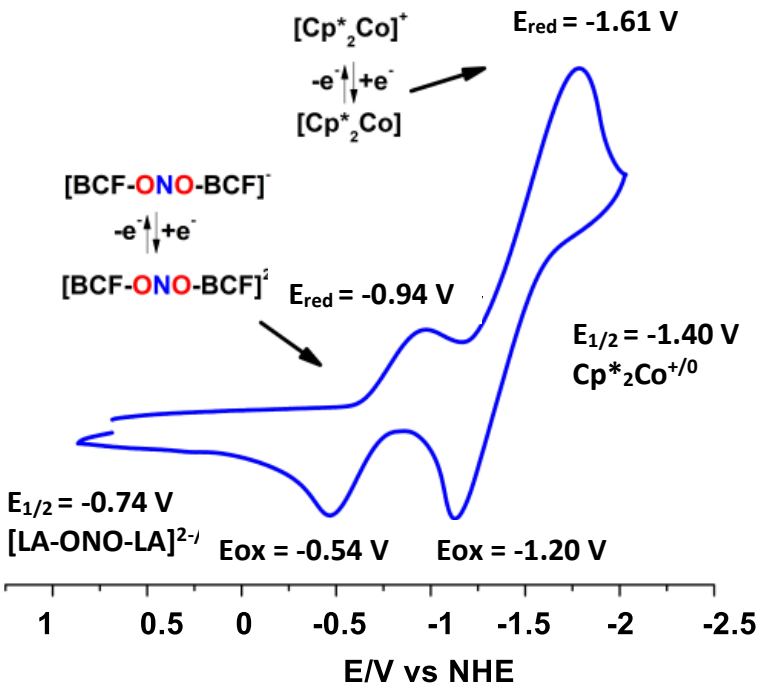

Figure 27. Cyclic voltammetry of $[Cp^*_2Co][(C_6F_5)_3B\text{-}ONO\text{-}B(C_6F_5)_3]$ (**3**) in fluorobenzene (4 mM) at 25 °C in presence of $[PPN][BAr^F_4]$ (0.1 M) with a scan rate of 100 mV/s.

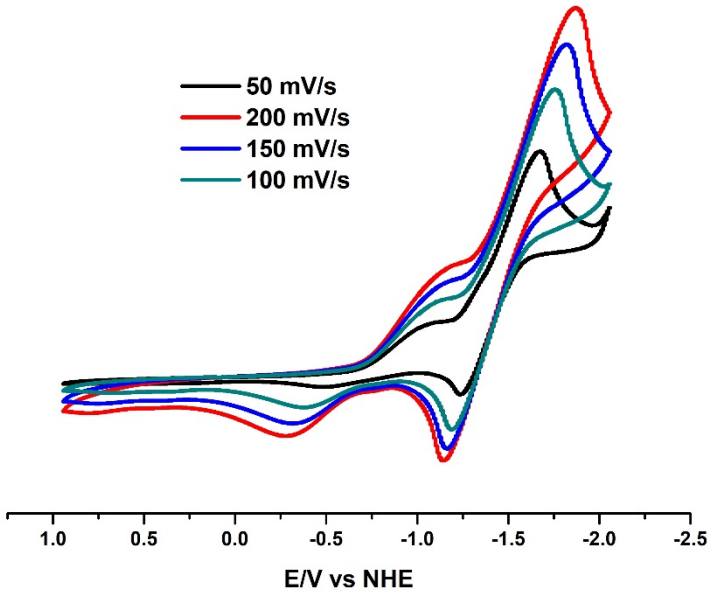

Figure 28. Cyclic voltammetry of $[Cp^*_2Co][(C_6F_5)_3B\text{-}ONO\text{-}B(C_6F_5)_3]$ (**3**) in fluorobenzene (4 mM) at 25 °C in presence of $[PPN][BAr^F_4]$ (0.1 M) with different scan rates.

14. Crystallographic details and additional structures

Single crystals of each compound $[Cp^*_2Co][NO_2]$ (**1**) (CCDC 2074366), $[Cp^*_2Co][(C_6F_5)_3B\text{-}ONO]$ (**2**) (CCDC 2074367), $[Cp^*_2Co][(C_6F_5)_3B\text{-}ONO\text{-}B(C_6F_5)_3]$ (**3**) (CCDC 2074368), $[Cp^*_2Co][(C_6F_5)_3B\text{-}ONO\text{-}B(C_6F_5)_3]$ (**4**) (CCDC 2074369), $[Cp^*_2Co][(C_6F_5)_3B\text{-}OCOCF_3]$ (**5**) (CCDC 2074370), [Cp*$_2$Co][BCF-F] (**6**) (CCDC 2074371) and $[(\eta^5\text{-}C_5Me_4CH_2\text{-}B(C_6F_5)_3)CoCp^*]$ (**7**) (CCDC 2074372) were mounted under mineral oil on a Mitegen micromount and immediately placed in a cold nitrogen stream at 100(2) K prior to data collection. Data for compounds **1**, **2** and **4** were collected on a Bruker D8 Quest equipped with a Photon100 CMOS detector and a Mo ImS source. Data for **3, 5, 6 and 7** were collected on a Bruker DUO equipped with an APEXII CCD detector and Mo fine-focus sealed source. A series of 0.5° φ- and ω-scans were collected with monochromatic Mo Kα radiation, λ = 0.7107 Åand integrated with the Bruker SAINT program. Structure solution and refinement was performed using the SHELXTL/PC suite and ShelXle. Intensities were corrected for Lorentz and polarization effects and an empirical absorption correction was applied using Blessing's method as incorporated into

the program SADABS. Non-hydrogen atoms were refined with anisotropic thermal parameters and hydrogen atoms were included in idealized positions unless otherwise noted. Further comments on disordered models:

$[Cp^*_2Co][NO_2]$ (1). The NO_2 group is disordered over two orientations. Similar displacement amplitudes were imposed on disordered sites overlapping by less than the sum of van der Waals radii. The disordered atoms were restrained to behave relatively isotropic. A partially occupied highly disordered fluorobenzene solvent molecule was removed from the model via the SQUEEZE routine in PLATON. There are several short contact distances between methyl groups of the cation and the oxygen atoms of the anion. O1···H8C_2 2.523 Å; O1···H8C_3 2.523 Å; O1···H9B_2 2.874 Å; O1···H9B_3 2.874 Å; O1···H10B 2.922 Å; O1···H10B_4 2.922 Å; O2···H9C 2.508 Å; O2···H9C_2 2.508 Å; O2···H6B_3 2.630 Å; O2···H6B_4 2.630 Å; O2···H10B 2.952 Å; O2···H10B_2 2.952 Å; (symmetry codes – 2: +x, 1-y, -1/2+z; 3: 1-x, 1-y, -1/2+z; 4: 1-x, +y, +z).

$[Cp^*_2Co][(C_6F_5)_3B\text{-}ONO\text{-}B(C_6F_5)_3]$ (4). One of the fluorobenzene solvent molecules in the lattice is disordered over two orientations. The phenyl rings were constrained to be ideal hexagons. The like C-F distances were restrained to be similar. The disordered atoms were restrained to behave relatively isotropic. Similar displacement amplitudes were imposed on disordered sites overlapping by less than the sum of van der Waals radii.

$[Cp^*_2Co][BCF\text{-}F]$ (6). Four highly disordered fluorobenzene solvent molecules were removed from the model via the SQUEEZE routine in PLATON.

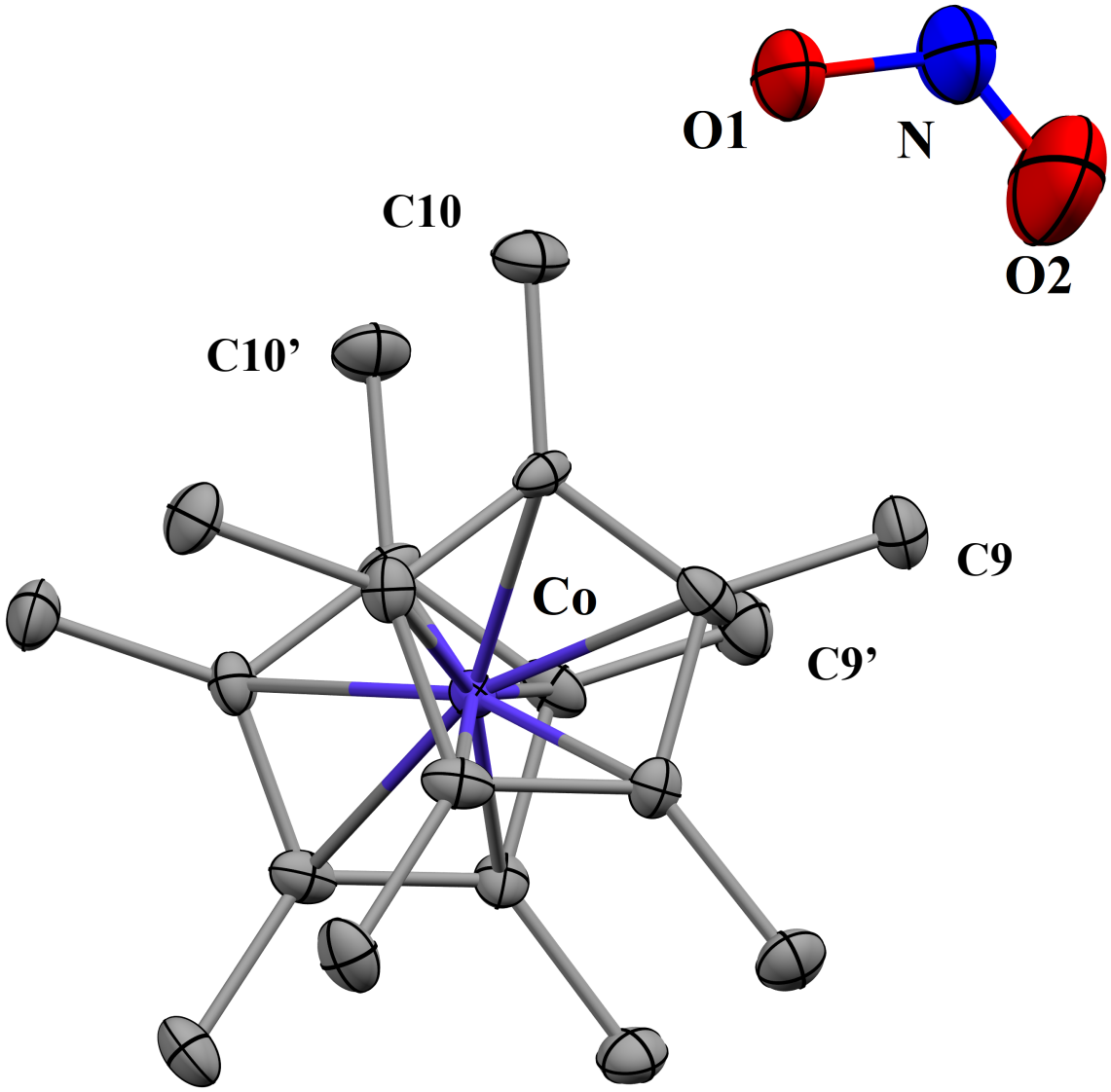

Figure 29. Molecular structure of $[Cp^*_2Co][NO_2]$ (**1**) (CCDC 2074366). The thermal ellipsoid plots are drawn at 50% probability level. Hydrogen atoms are omitted for clarity. Selected bond distances (Å) and angles (°): N-O1 1.110(8), N-O2 1.239(6), O1-N-O2 120.6(6). There are several short contact distances between methyl groups of the cation and the oxygen atoms of the anion. O1···H8C_2 2.523 Å; O1···H8C_3 2.523 Å; O1···H9B_2 2.874 Å; O1···H9B_3 2.874 Å; O1···H10B 2.922 Å; O1···H10B_4 2.922 Å; O2···H9C 2.508 Å; O2···H9C_2 2.508 Å; O2···H6B_3 2.630 Å; O2···H6B_4 2.630 Å; O2···H10B 2.952 Å; O2···H10B_2 2.952 Å.

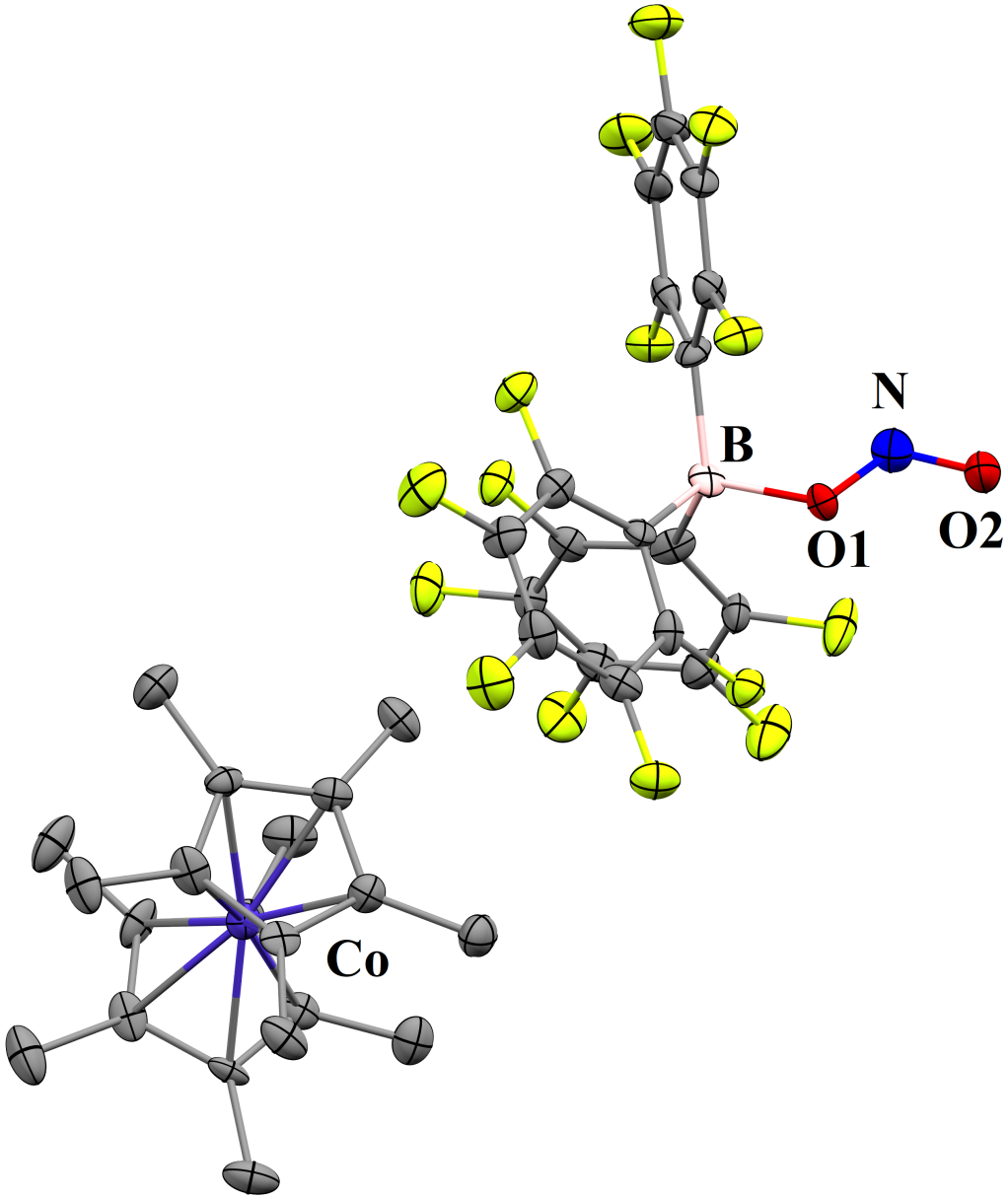

Figure 30. Molecular structure of $[Cp^*_2Co][(C_6F_5)_3B\text{-}ONO]$ (**2**) (CCDC 2074367). The thermal ellipsoid plots are drawn at 50% probability level. Hydrogen atoms are omitted for clarity. Selected bond distances (Å) and angles (°): N-O1 1.337(10), N-O21.200(10), O1-B 1.527(11),O1-N-O2 112.2(7), B-O1-N 113.6(7).

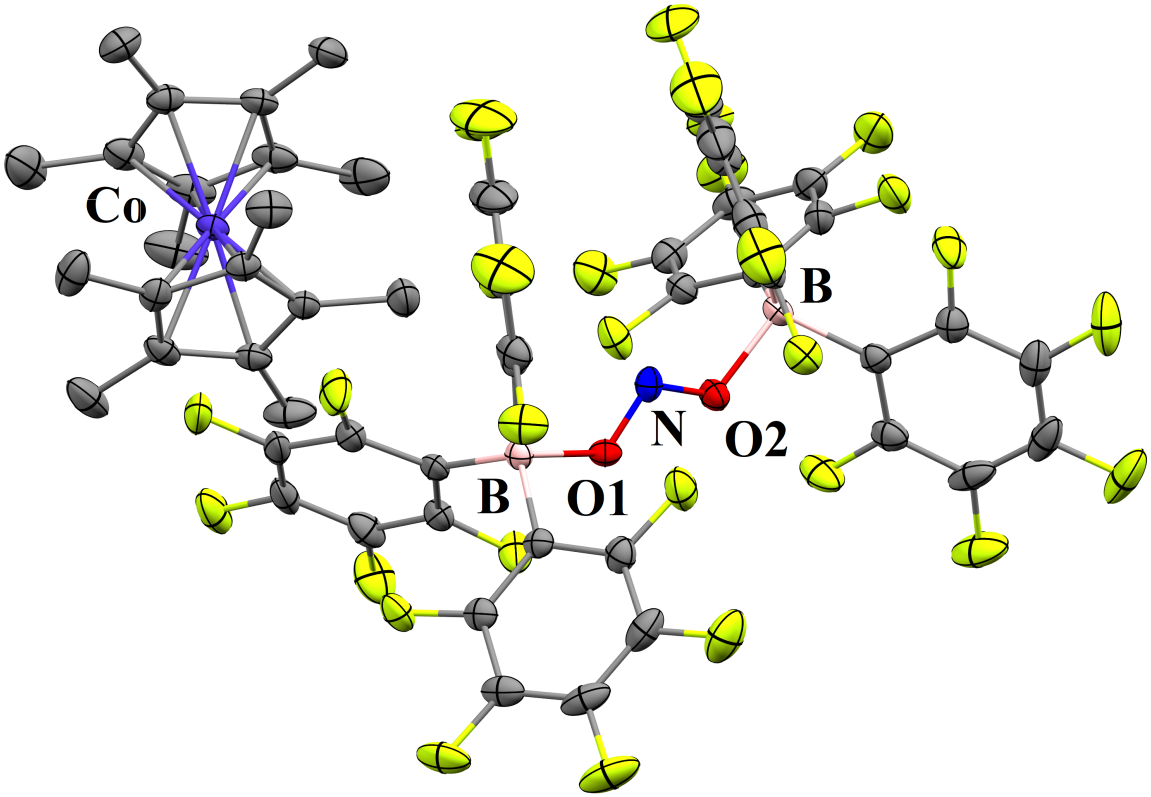

Figure 31. Molecular structure of $[Cp^*_2Co][(C_6F_5)_3B\text{-}ONO\text{-}B(C_6F_5)_3]$ (**3**) (CCDC 2074368). The thermal ellipsoid plots are drawn at 50% probability level. Hydrogen atoms are omitted for clarity. Selected bond distances (Å) and angles (°): N-O1 1.261(2), N-O21.225(2), O1-B 1.603(3), O2-B 1.628(3), O1-N-O2 109.30(17), B-O1-N 116.78(16), B-O2-N 117.41(16).

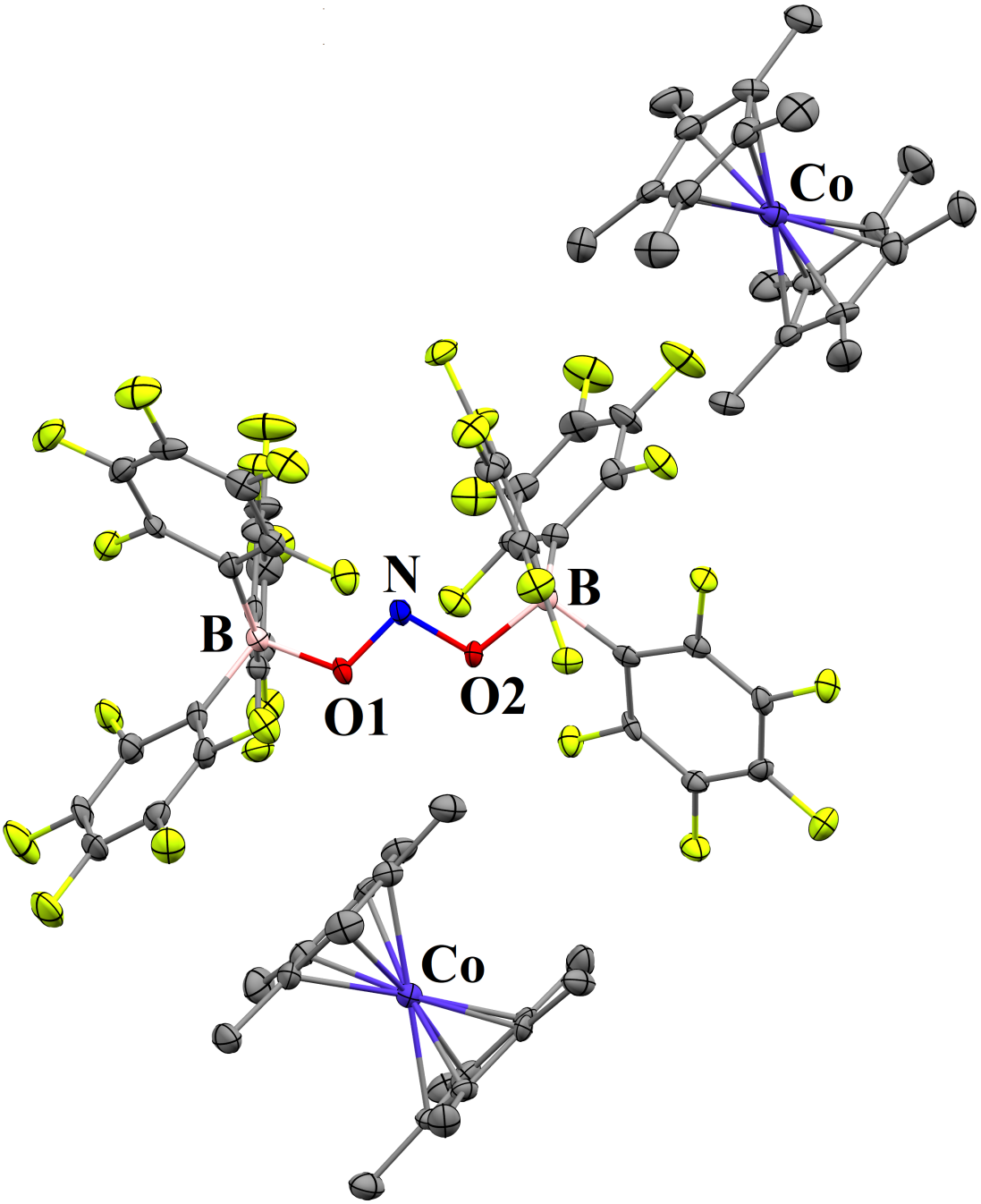

Figure 32. Molecular structure of $[Cp^*_2Co]_2[(C_6F_5)_3B\text{-}ONO\text{-}B(C_6F_5)_3]$ (**4**) (CCDC 2074369). The thermal ellipsoid plots are drawn at 50% probability level. Hydrogen atoms are omitted for clarity. Selected bond distances (Å) and angles (°): N-O1 1.385(7), N-O21.373(7), O1-B 1.488(9), O2-B 1.490(9), O1-N-O2 103.5(5), B-O1-N 109.7(5), B-O2-N 109.7(5).

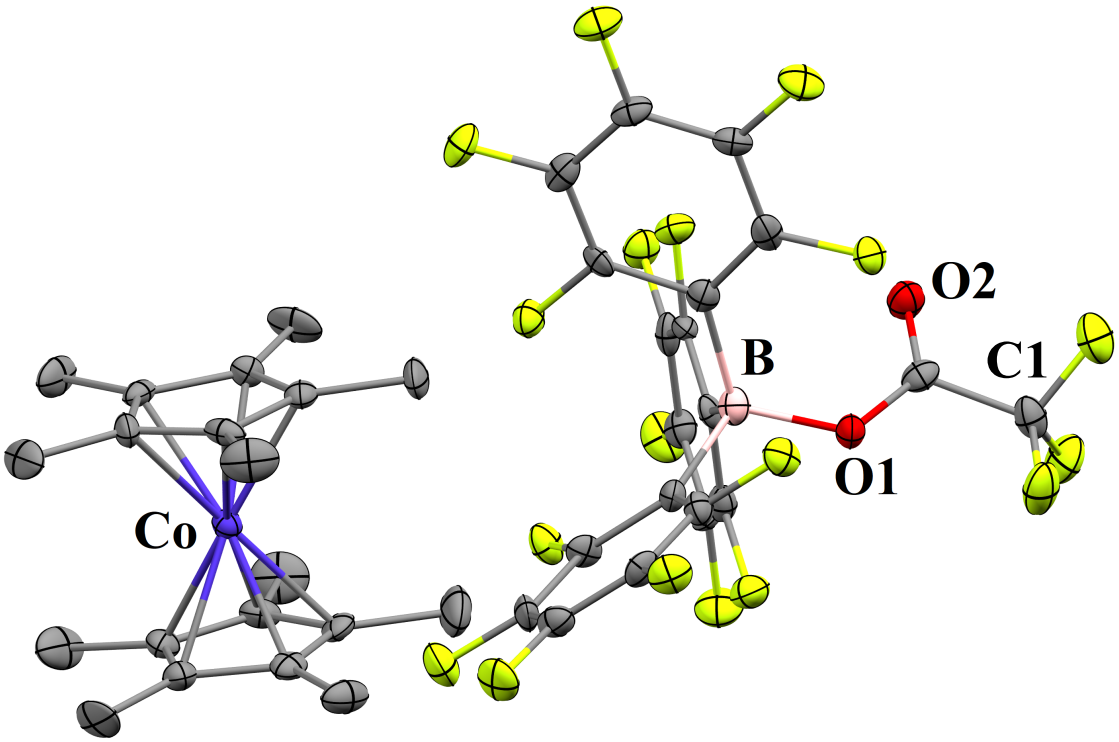

Figure 33. Molecular structure of $[Cp^*_2Co][(C_6F_5)_3B\text{-}OC(O)CF_3]$ (**5**) (CCDC 2074370). The thermal ellipsoid plots are drawn at 50% probability level. Hydrogen atoms are omitted for clarity. Selected bond distances (Å) and angles (°): B-O1 1.525(6), C-O1 1.308(5), C-O2 1.218(5), B-O1-C 120.3(4).

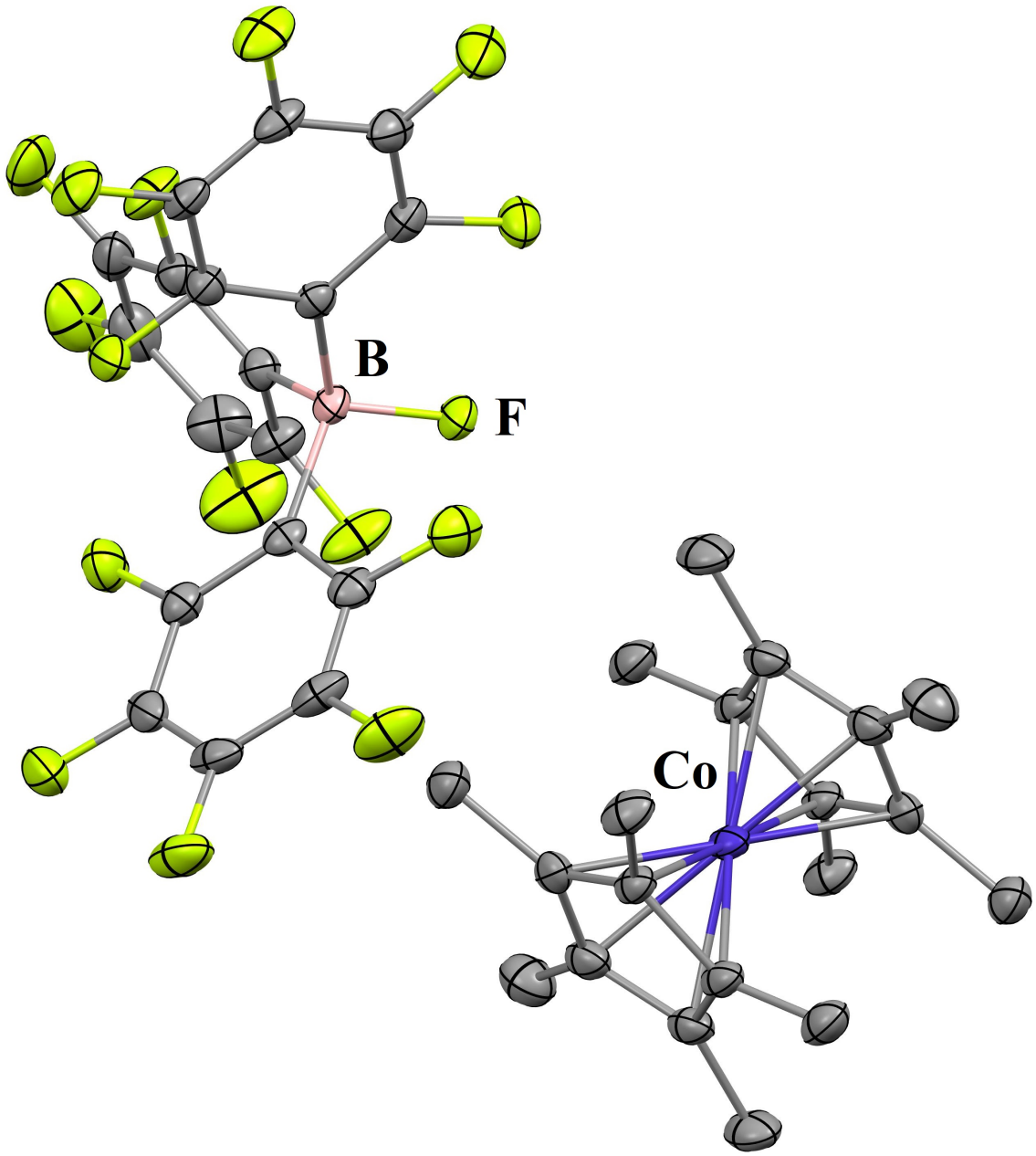

Figure 34. Molecular structure of $[Cp^*_2Co][(C_6F_5)_3B\text{-}F]$ (**6**) (CCDC 2074371). The thermal ellipsoid plots are drawn at 50% probability level. Hydrogen atoms are omitted for clarity. Selected bond distances (Å) and angles (°): B-F 1.427(3).

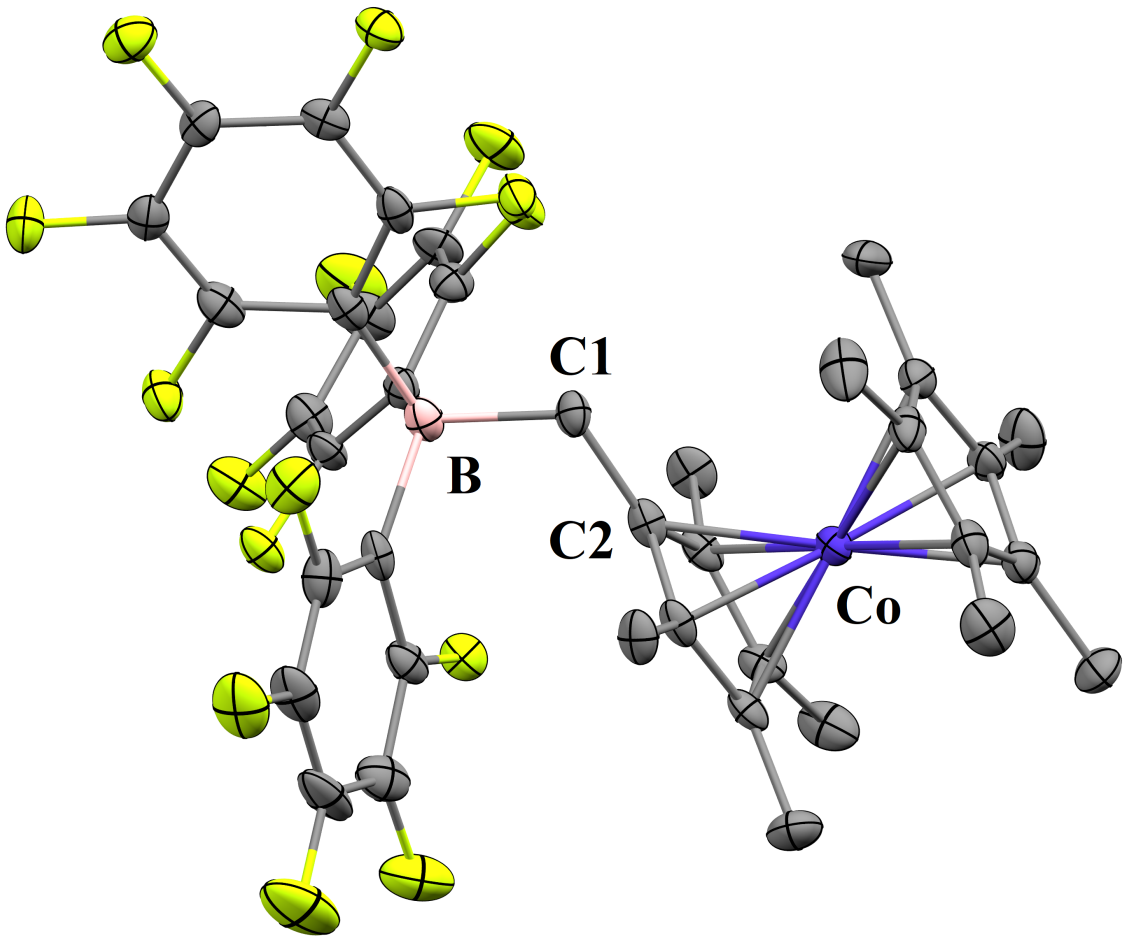

Figure 35. Molecular structure of [(η^5-$C_5Me_4CH_2$-$B(C_6F_5)_3$)CoCp*] (**7**) (CCDC2074372). The thermal ellipsoid plots are drawn at 50% probability level. Hydrogen atoms are omitted for clarity. Selected bond distances (Å) and angles (°): B-C1 1.669(5) B-C1-C2 120.4(3).

15. XAS

N K-edge XAS measurements for all compounds were collected on beamline 10-1, equipped with a 31-pole wiggler source, a 600 lines/mm spherical grating monochromator and 30 μm entrance and exit slits. Samples were prepared as solids in an inert-atmosphere drybox, ground to a fine powder and spread in a thin layer on carbon tape affixed to an Al sample rod. Data were measured by monitoring fluorescence using a transition edge sensor (TES) operated under typical conditions as described previously.[8] Raw TES data was processed into pulse heights via a matched filter,[9] and these pulse heights were calibrated by measuring the non-resonant emission from a blended powder of graphite, boron nitride, iron oxide, nickel oxide, and copper oxide. The signal was normalized to incident photon flux with a gold-grid reference monitor and incident beam energy was calibrated to the Ni L_3 second order transition at 426.35 eV measured in a reference channel. The nitrogen PFY-XAS was created by windowing the measured emission between 360 and 420 eV. Samples were maintained at room temperature under an ultra-high vacuum (10^{-9} Torr) during collection. Data were collected from 380.0 eV to 485.0 eV. Processing was carried out using PyMCA.[10] Background subtraction was achieved with E_0 set at 410 eV, by fitting a line to the pre-edge region below 395 eV and subtracting from the entire spectrum. The post edge region from 420.0 eV to 485.0 eV was set to a flattened polynomial and normalized to 1.0. Raw data were smoothed in Igor using a 4^{th} order Savitsky-Golay smoothing algorithm.

16. EPR Spectroscopy

X-band cwEPR experiments were carried out with a Bruker E500 spectrometer in an ER 4103TM resonator. Microwave powers of 0.2mW (96K) or 2mW (for room temperature) and a modulation amplitude of 1 G were used to carry out the measurements. For measurements at 96K, the samples were cooled in a steady flow of cold gaseous nitrogen and the temperature controlled by a variable temperature unit. Q-band field swept echoes were measured on a Bruker E580 spectrometer equipped with a FlexLine Cryogen-Free VT System at 10K using a three-pulse echo sequence ($\pi/2$-τ- $\pi/2$-T- $\pi/2$-τ) with four step phase cycling. Microwave pulses were generated using a 10W solid state amplifier with

a π/2 pulse corresponding to 14-16 ns. The pseudo-modulation algorithm (with 4G pseudo modulation) was used to generate the first derivative spectra using Xepr (Bruker Biospin, Karlsruhe, Germany. The EPR simulations were carried out using EasySpin.[11]

Table 2. Experimental[a] and DFT-calculated[b] spin Hamiltonian parameters and fitting parameters for ^{14}N–**4**.

Collection Mode	CW X-band (9.3886 GHz), 298 K	CW X-band (9.2710 GHz), 100 K	FSE Q-band (33.9544 GHz), 10 K	DFT
g_x	–	1.991	1.996	2.002
g_y	–	1.996	1.998	2.005
g_z	–	1.996	2.003	2.007
g_{iso}	2.005[c]			2.005
^{14}N A_x (MHz)	–	122	126	121.4
^{14}N A_y (MHz)	–	4.2	5.0	–1.8
^{14}N A_z (MHz)	–	5.7	5.0	0.0
^{14}N A_{iso} (MHz)	44	–	–	39.9
H-strain (x) (MHz)	4.7	5.3	12.8	–
H-strain (y) (MHz)	3.6	4.9	38.8	–
H-strain (z) (MHz)	6.5	5.0	18.2	–
Linewidth (MHz)	0.5	1.5	0.6	–

[a]Obtained from EasySpin simulations. [b]Details given below in **18**. [c]Obtained by fitting one g-value. [d]Obtained by averaging anisotropic g-values.

Table 3. Experimental[a] spin Hamiltonian parameters and fitting parameters for ^{15}N–**4**.

Collection Mode	**CW X-band (9.7249 GHz), 298 K**	**CW X-band (9.3246 GHz), 100 K**	**FSE Q-band (33.9075 GHz), 10 K**
g_x	–	2.003	1.995
g_y	–	2.003	1.997
g_z	–	2.011	2.003
g_{iso}	2.005[c]		
^{15}N A_x (MHz)	–	170	178
^{15}N A_y (MHz)	–	0.0	5
^{15}N A_z (MHz)	–	0.0	5
^{15}N A_{iso} (MHz)	62	–	–
H-strain (x) (MHz)	6.7	0.0	24
H-strain (y) (MHz)	8.5	20	70
H-strain (z) (MHz)	1.9	20	0.0
Linewidth (MHz)	0.5	1.6	0.8

[a]Obtained from EasySpin simulations. [b]Obtained by fitting one g-value. [c]Obtained by averaging anisotropic g-values.

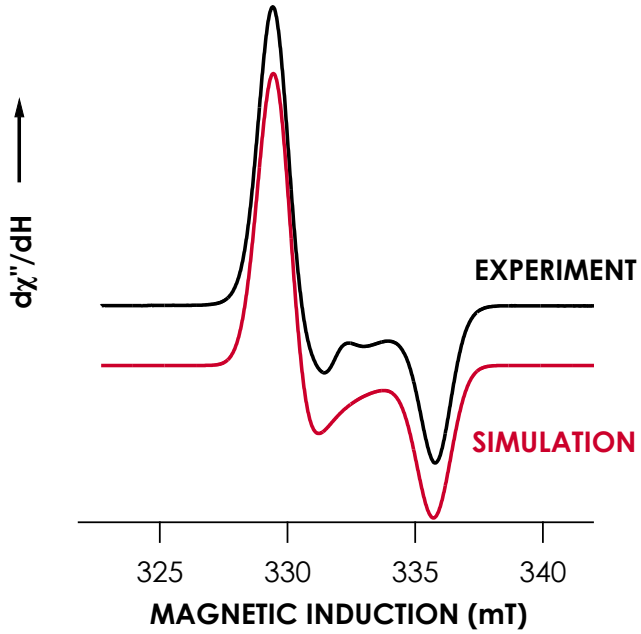

Figure 36. 100 K frozen solution CW X-band (9.2346 GHz) EPR spectrum of ^{15}N–**4**. Experimental data are in black, EasySpin simulation is in red.

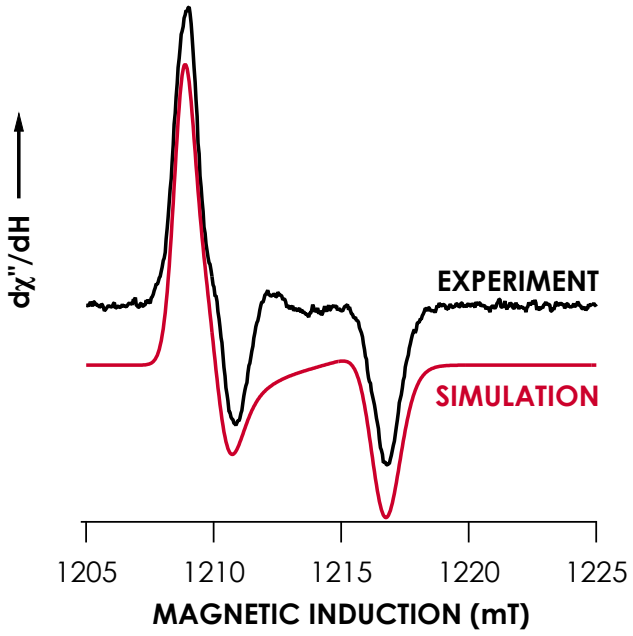

Figure 37. 10 K frozen solution FSE-detected Q-band (33.9075 GHz) EPR spectrum of ^{15}N–**4**. Experimental data are in black, EasySpin simulation is in red.

17. Quantum Chemical Calculations

All electronic structure and spectroscopic calculations were performed using the ORCA computational chemistry package.[12] Crystal structure coordinates were used for TDDFT[13] calculations of N K-edge XAS utilizing the B3LYP[14] functional, with the zeroth-order regular approximation for relativistic effects (ZORA)[15-17] as implemented by van Wüllen.[18] The RIJCOSX algorithm was used to speed the calculation of Hartree−Fock exchange.[19] Special integration accuracy, Grid7[20] was used for nitrogen and oxygen while the scalar relativistically recontracted ZORA-def2-TZVP(-f) basis set[16] with ORCA Grid4 was used for all other atoms. Solvation was modeled with CPCM in an infinite dielectric.[21] Calculated excitation energies for pre-edge and edge features were plotted against experimental energies for the B3LYP functional. This correlation was used to shift the calculated energy of the spectra and produce calculated N K-edge spectra that nicely reproduce experimental spectra, as described previously.[22] Single point DFT solutions were used to predict EPR properties using coupled perturbation Kohn−Sham theory for the g-matrix, and the SOC operator was treated by the spin−orbit mean-field approximation.[23] Fermi contact terms (A_{iso}) and spin–dipole contributions to the first-order hyperfine coupling contributions for ^{14}N were obtained as expectation values over the B3LYP ground state spin density.[24]

Reaction coordinates were calculated using the same functional and basis set combinations as described above. Stringent geometry convergence criteria were set in ORCA using !VeryTightOpt. Transition state searches for the reaction of NO_2^{2-} with NO were carried out in ORCA using a quasi-Newton like Hessian mode-following algorithm.[25-33] Initial guesses for transition states were obtained by scanning along chemically plausible reaction vectors, e.g. contraction of the N–N interatomic distance in the case of attack of NO on NO_2^-, and elongation of the N–N interatomic distance during the scission of $[ON(NO)O]^{2-}$ to yield NO^- and NO_2^-. In the former case, a transition state was identified, optimized, and subjected to numerical frequency calculations to obtain its Gibbs energy. In the latter case, the transition state was approximated as the point of avoided crossing between singlet and triplet states when scanning the elongation of the N–N bond of the $[ON(NO)O]^{2-}$ intermediate. The Gibbs energies of the singlet and triplet states at this

crossing point were evaluated by numerical frequency calculations and found to lie within 0.5 kcal/mol of one another. Thermodynamics for the complete reaction of **4** with three equivalents of NO were obtained via numerical frequency calculations, with fluorobenzene solvation modeled by specifying its dielectric (5.42) and refractive index (1.465) in the CPCM correction.

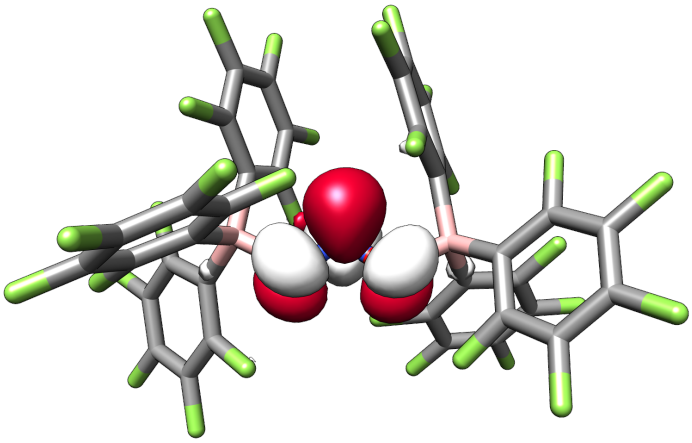

Figure 38. LUMO of monoanion $[(C_6F_5)_3B\text{-}ONO\text{-}B(C_6F_5)]^-$ in **3**.

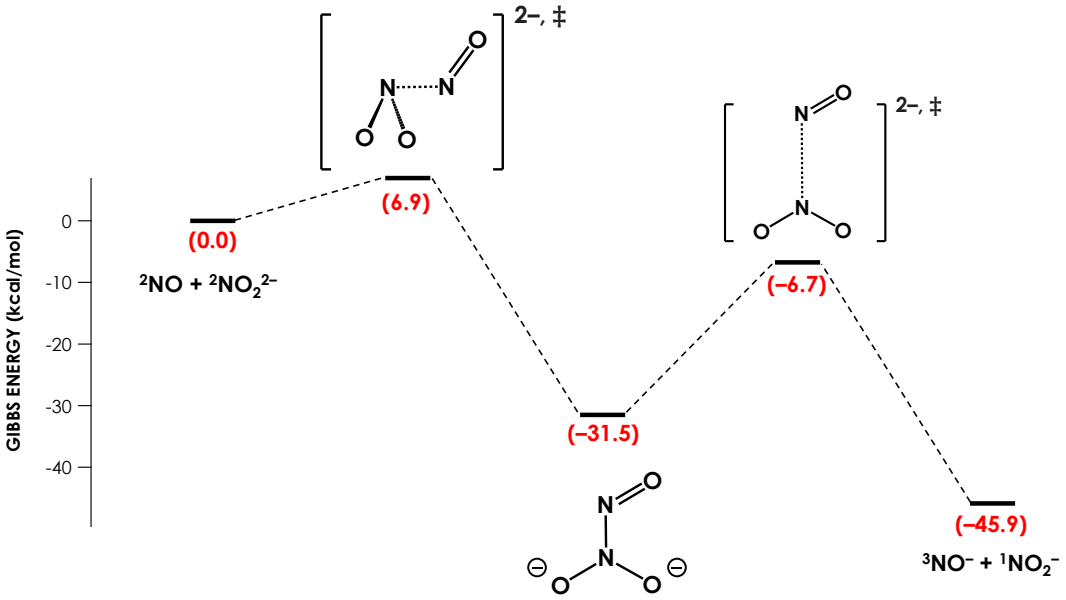

Figure 39. DFT-calculated (B3LYP/ZORA-def2-TZVP(-f), CPCM with infinite dielectric) reaction coordinate for the reaction of NO with NO_2^{2-}. Values in red are Gibbs energies in kcal/mol relative to NO + NO_2^{2-}.

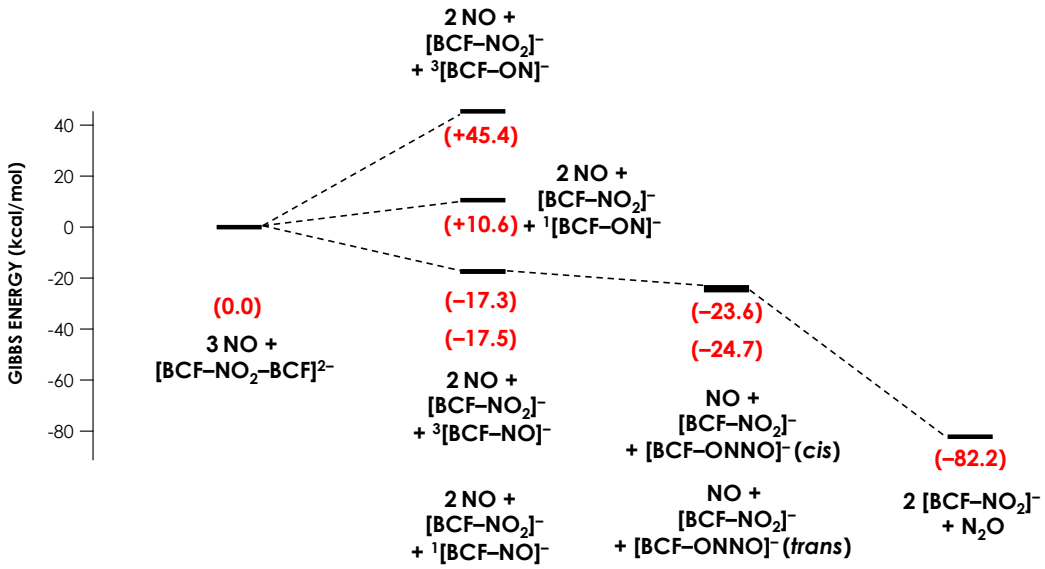

Figure 40. DFT-calculated (B3LYP/ZORA-def2-TZVP(-f), CPCM used to model fluorobenzene) reaction coordinate for the reaction of **4** with 3 equivalents of NO. Values in red are Gibbs energies in kcal/mol relative to **4** + 3 NO. Transition state searches were not carried out (BCF = $B(C_6F_5)_3$).

Crystallographic Coordinates Used for Electronic Structure Calculations of Monoanion **3** (*S* = 0)

N	0.00000	0.00000	0.00000
F	3.47912	-0.29620	-0.87635
F	-1.85206	0.68953	2.19918
F	3.93437	-3.48981	0.99889
F	-0.38231	-1.83706	-1.99315
F	0.91746	3.69786	0.16149
F	-0.02063	-3.83738	2.29492
F	-3.13698	4.00929	-1.37516
F	0.38938	-0.90754	2.78126
F	0.47884	1.18130	-2.57680
F	0.53171	2.30400	-4.97523
O	1.14170	-0.39925	0.21273
F	-3.61103	3.13878	1.36023
F	5.13360	-3.44836	3.34664
F	3.06584	-5.19314	-3.15132
F	-1.18495	4.30208	-5.62330
F	4.97999	-3.42372	-3.98971
F	-3.44808	0.86233	-2.25625

F	-3.01510	5.15480	-3.78194
O	-0.00000	1.26146	0.00000
F	1.47289	-4.58330	-1.15571
F	4.03982	-2.10381	5.45487
F	-3.58642	-1.28954	2.72159
F	5.12287	-0.97856	-2.84335
F	1.62649	-0.91208	5.15207
F	-3.47412	5.30168	2.88252
F	1.06046	5.84257	1.71438
F	-2.70787	-3.07776	-2.36148
F	-2.31272	-5.09731	1.86681
F	-3.69896	-4.73808	-0.44348
F	-5.17102	-1.06988	-1.69863
F	-1.14318	6.68255	3.11454
F	-5.27070	-2.17883	0.76903
C	3.31411	-2.80421	1.97092
C	2.32866	-2.37251	-0.92866
C	-2.41925	3.74499	1.45650
C	2.10117	-2.14007	1.75869
C	-1.23418	3.75946	-4.39427
C	-1.33804	3.24656	0.72667
C	4.18753	-1.84721	-2.42519
C	3.16330	-3.97671	-2.58149
C	3.31561	-1.51850	-1.42160
C	-0.09406	5.14376	1.64107
C	-2.35015	4.86908	2.25127
C	4.11701	-3.08737	-3.01620
C	-1.29626	2.56494	-1.82746
C	3.96683	-2.81231	3.20788
C	-0.09349	-2.74312	0.17388
C	2.32414	-3.62093	-1.56606
C	-0.40415	2.17367	-2.81011
C	-0.18201	4.01683	0.85354
C	-2.14492	4.17006	-3.48003
C	-0.84312	-2.61633	-0.98686
C	-0.64697	-3.59427	1.11311
C	1.57609	-1.53420	2.87075
C	-1.20003	5.56900	2.35220
C	-2.56024	0.88594	-0.04275
C	-2.17265	3.58394	-2.23176
C	-3.41910	0.37008	-1.01204
C	3.40434	-2.16172	4.25464
C	-0.34112	2.73231	-4.07900
C	2.18462	-1.51684	4.12217
C	-2.67556	0.27205	1.19468
C	-2.03222	-3.25539	-1.20744

B	1.35839	-2.01291	0.30553
C	-3.54861	-0.74065	1.49883
C	-1.84577	-4.26589	0.92788
C	-4.33044	-0.64403	-0.74638
C	-4.39373	-1.20403	0.52037
B	-1.38878	1.97784	-0.31573
C	-2.54067	-4.08917	-0.23631

Crystallographic Coordinates Used for Electronic Structure Calculations of Dianion **4** (*S* = ½)

N	0.00000	0.00000	0.00000
F	-6.24197	-0.96363	-0.45204
F	-2.29021	-3.38170	-3.24732
F	-6.78876	-2.29751	-2.76017
F	-3.74795	-0.78023	0.42728
F	1.48897	-2.93404	-0.50575
F	-4.78894	-3.56800	-4.08618
F	0.78481	3.43181	-1.67577
F	0.61982	6.05778	-1.94198
F	0.51543	-0.93374	-5.44487
F	1.75881	0.75390	-2.04381
F	2.67882	-0.45238	1.93923
F	2.95842	-1.96616	-4.83078
F	-0.74332	2.69297	2.83007
F	3.77114	2.40905	1.91881
F	0.78911	7.68657	0.24376
F	-0.93428	-3.05495	4.06255
F	-0.87456	-6.44836	0.81466
F	0.38758	-0.52430	5.99334
F	2.28477	-1.52856	4.32699
F	4.14357	0.41619	-3.09669
F	-0.77056	-5.69456	3.42911
F	6.16470	2.19844	0.76423
F	6.37980	1.19000	-1.76801
F	1.31201	6.59224	2.68102
F	-1.39248	-0.81060	-3.60816
F	-1.11042	-4.62263	-1.09437
F	3.41105	-2.91018	-2.31429
F	1.54552	3.98945	2.96919
F	-1.23946	-1.22240	2.19018
F	-1.12045	1.59836	5.20118
O	-1.25207	-0.32235	-0.45841
O	0.00000	1.38401	0.00000
C	2.18939	-2.44984	-2.63883
C	-3.92550	-1.44315	-0.73660

C	1.16558	-2.43396	-1.70784
C	-5.53375	-2.22740	-2.30875
C	-5.23800	-1.53707	-1.16381
C	-2.84528	-1.99392	-1.39900
C	-0.22285	-1.41797	-3.24544
C	1.76010	0.13747	2.71786
C	-0.10579	-1.95269	-1.98006
C	5.06966	1.79690	0.10356
C	-1.07807	-4.17865	0.18205
C	-3.21894	-2.72076	-2.52148
C	-1.14516	-2.80965	0.41592
C	1.98449	-1.95342	-3.89920
C	1.25087	4.42271	1.72021
C	3.80286	1.90542	0.64948
C	1.13831	5.79681	1.60270
C	0.07972	1.67166	3.15681
C	-4.51021	-2.84065	-2.97670
C	-0.94809	-5.14263	1.14766
C	-1.12805	-2.50679	1.76631
C	0.75083	-1.42932	-4.20220
C	0.77903	5.52333	-0.71626
C	1.55496	-0.46453	3.94922
C	5.18575	1.29354	-1.16980
C	-0.90219	-4.76077	2.46015
C	1.04059	1.24472	2.26775
C	2.62388	1.56401	0.02367
C	0.59505	0.03272	4.78325
C	1.07147	3.52852	0.67548
C	0.86723	4.16225	-0.52863
C	-0.98926	-3.43543	2.76831
C	4.02735	0.93465	-1.84235
C	2.80941	1.07475	-1.26118
C	0.89337	6.35474	0.37560
C	-0.14125	1.10719	4.38547
B	-1.29263	-1.75973	-0.83813
B	1.17976	1.88938	0.75030

Optimized Coordinates for NO_2^{2-} ($S = ½$)

N	0.00000	0.00000	0.00000
O	-1.25207	-0.32235	-0.45841
O	0.00000	1.38401	0.00000

Optimized Coordinates for NO ($S = {}^1/_2$)

N	0.00000000000000	0.00000000000000	0.01934215626724
O	0.00000000000000	0.00000000000000	1.16471784373276

Optimized Coordinates for NO_2^{2-} + NO^- N–N Bond Formation Transition State (S = 0)

N	0.53198838572838	-0.36360043323355	1.16829712234054
N	0.03585079616220	0.31630176106269	-0.53943440935940
O	0.88192121596525	0.48382315179598	1.95984959433541
O	1.29029202266831	-0.05947272661612	-0.87830498581944
O	-0.87175242052419	-0.48805175300900	-1.06658732149709

Optimized Coordinates for $[ON(NO)O]^{2-}$ Intermediate (S = 0)

N	0.29077451052986	0.11356146203501	-0.03203253749150
N	0.05582617649056	-0.08593656365394	-1.28252737665771
O	-0.67749122847309	-0.28619500252046	0.79962988308439
O	0.98499500758808	0.29112452548055	-2.14680959815610
O	-1.03059446613541	-0.63080442134116	-1.74445037077908

Optimized Coordinates for $[ON(NO)O]^{2-}$ N–N Bond Scission Transition State (S = 1)

N	0.18220696740290	0.30174227892456	0.15795891461386
N	0.14176726986834	-0.37675969458268	-1.43292125049194
O	-0.57701423108393	-0.34046372058543	0.92796053923199
O	0.96143029292428	0.31143811114967	-2.19226239222211
O	-1.08488029911157	-0.49420697490609	-1.86692581113174

Optimized Coordinates for NO_2^- (S = 0)

N	-0.08853227897778	0.07920274837727	-0.03241358870207
O	-1.19852551172152	-0.34751877449469	-0.43880620079409
O	0.03498779069930	1.32997602611743	0.01280978949617

Optimized Coordinates for NO^- (S = 1)

N	-0.08910721991365	0.07893169400440	-0.03262408705632
O	-1.19785632060467	-0.34716463489847	-0.43856119540312

Optimized Coordinates for **4** ($S = {}^1/_2$)

N	0.08312017153045	0.03714727201208	0.02305913624691
F	-6.23457277264406	-0.96851657405364	-0.78746704475392
F	-2.05867180024286	-3.39587571647753	-3.27515555316275
F	-6.66701097882427	-2.76660324196961	-2.79309599337205
F	-3.76960289528530	-0.47367456870273	0.07292697412441

F	1.22987908326009	-3.25678947936802	-0.08597340966515
F	-4.54122667520063	-3.97522403479232	-3.99562197482441
F	0.35935927267028	3.59827387586150	-1.51391734056143
F	-0.35702395361738	6.16415001772821	-1.40833628963605
F	1.43593734825198	-0.85121178704817	-4.94329022376450
F	1.54861460172486	1.16204129727405	-2.28253374716068
F	3.29631540576151	-0.25070170337510	1.63617226082316
F	3.63313892464235	-2.10713769552569	-3.91733082808309
F	-0.45865267831020	2.39910345267536	2.85231047615556
F	4.09634013359543	2.45664087856796	1.51260095870813
F	0.07464066265144	7.62987097730768	0.85022121325055
F	-2.26259920773607	-2.85914794237483	4.03309027806845
F	-1.85826198898766	-6.35173942190930	0.88646227222248
F	1.23633217953030	-0.81441902989616	5.79986783462127
F	3.19278030635128	-1.44171281302661	4.00651218581648
F	3.79198178184939	0.87146134070016	-3.66666485714121
F	-2.41172579604953	-5.51500663376498	3.43076356166794
F	6.34199511350888	2.14298693875896	0.08936936393613
F	6.22069513701419	1.33284491418550	-2.51200499321239
F	1.25980265456652	6.45392779835804	3.01248654437090
F	-0.86389122529960	-0.81761967270117	-3.58920403424320
F	-1.26729526207277	-4.57641113256779	-1.01156498380583
F	3.48207928578611	-3.27450333092478	-1.45164141306991
F	1.96650433622487	3.89265686008176	2.94844260584895
F	-1.65700268709850	-1.06498117328527	2.16126111260938
F	-0.54236598783005	1.17196592640511	5.21151802988427
O	-1.15037027700771	-0.26649062841496	-0.48906460750912
O	0.11425915484213	1.40272398024329	0.03795373112580
C	2.39381582399311	-2.68803136757362	-1.99004996934914
C	-3.88664851910668	-1.30524436031309	-0.98242304124072
C	1.19446665638514	-2.65964968747391	-1.29688256560408
C	-5.41480027270365	-2.47239080294265	-2.40654702639600
C	-5.18710819331049	-1.56379592264156	-1.38983908097987
C	-2.75885518875308	-1.88857798599504	-1.55998702607420
C	0.17905101274055	-1.47000012817921	-3.02434669846914
C	2.33762056176736	0.17889439704477	2.48822259394526
C	0.04138293232901	-2.04872023881056	-1.77006433067599
C	5.14587223258326	1.89514913772413	-0.48037908949081
C	-1.50421265345525	-4.09696479707574	0.23155712931208
C	-3.04362100700911	-2.76503595876979	-2.60126136265638
C	-1.43822670545243	-2.72821873252857	0.46221065478735
C	2.47925826041765	-2.08990988724103	-3.23158612312894
C	1.37025985741136	4.38755004824279	1.84047004894647
C	3.96825093875863	2.03684696619939	0.23102363186869
C	1.02819748021109	5.73170487562039	1.89973642533998
C	0.49039154984838	1.46551487571241	3.09104893168398

C	-4.33136201665184	-3.07731709516529	-3.01504795046163
C	-1.81144164570721	-5.04036394778553	1.19216348679230
C	-1.69169148281907	-2.35496905986326	1.77606776177774
C	1.35579918165591	-1.47395172300563	-3.75370009294674
C	0.20205284601816	5.58222548875460	-0.32976662072217
C	2.29144178932620	-0.48600352881746	3.70622051007071
C	5.09077856595418	1.48028662500475	-1.79963811763944
C	-2.08018814757002	-4.62079340469673	2.48329158792104
C	1.46214834553090	1.19486535432800	2.13442943520326
C	2.70629901596246	1.75463467077494	-0.27846551845425
C	1.31334935826549	-0.16429497303109	4.62721032031179
C	1.10756698460729	3.57363257160544	0.74636930156054
C	0.56060944460530	4.24247120230874	-0.34656984975781
C	-2.00822633264389	-3.27100163525556	2.77593421000594
C	3.85660152799460	1.23906871880352	-2.37348704902079
C	2.69751744774099	1.38614488982654	-1.61918747895607
C	0.42556716428958	6.33358220409495	0.81006122827338
C	0.40439550459950	0.83017165027845	4.31605659972236
B	-1.27534951149103	-1.70667512021415	-0.83762254851892
B	1.35907582612196	1.93806773107456	0.66112643750514

Optimized Coordinates for $[(C_6F_5)_3B–NO]^-$ ($S = 0$)

O	-0.89592779924520	1.65534779970897	-0.04606206223837
F	0.43919157585345	3.52640010843667	-1.53060717382205
F	-0.35129836972405	6.08834407479481	-1.42563231292209
F	1.72311384599222	0.47145584128446	-2.04679745003667
F	3.31723737903613	-0.28889650922385	1.54883625038593
F	-0.45290212175722	2.29460126892343	2.85961341730627
F	3.98904932378142	2.90479677744850	1.34804323753377
F	0.00107354064383	7.54400226380425	0.85204765774327
F	1.34273926316563	-0.92062887181292	5.74037306007821
F	3.26264421632659	-1.51183714753376	3.90522176264099
F	4.02060276457824	0.20795163364578	-3.35260028433086
F	6.25416826634722	2.68375112557339	-0.00894673429322
F	6.31939900165127	1.30236153883159	-2.38402217720683
F	1.14519589356694	6.37495713844829	3.03952884835786
F	1.88882703487051	3.82277742827785	2.97792879130950
F	-0.47684407361105	1.04616148922207	5.20564363578750
N	0.17663001123468	1.08880497756411	0.05064971048900
C	2.36392615848245	0.10937252174705	2.41972490825257
C	5.13450464821748	2.13409711375818	-0.50984308268676
C	1.31302552774836	4.31925920128618	1.86062161064927
C	3.93698900103041	2.24465487565766	0.17066585318475
C	0.94858363399648	5.65583933895271	1.91918728831549
C	0.50607268302633	1.37086574913667	3.07206419238737

C	0.19245169497627	5.50900181572128	-0.33924129638510
C	2.35006144870783	-0.56377918282446	3.63340564611170
C	5.17001803168930	1.43752761524569	-1.70552099689085
C	1.46870455475732	1.12320927498741	2.09632910506907
C	2.73629244468193	1.69689338690020	-0.26553861365110
C	1.38615718942428	-0.25967237985480	4.57677659470249
C	1.10654352571850	3.51505027405168	0.74820711439430
C	0.57896990152147	4.17779754581942	-0.35420168316242
C	3.99935849657302	0.88395743675021	-2.19129904643326
C	2.81446640767374	1.03104320899100	-1.48075272503825
C	0.37062955925088	6.25432435807526	0.81363484754579
C	0.45640825300596	0.72467708585748	4.29394699037841
B	1.39986708680724	1.90943982234744	0.64953511647423

Optimized Coordinates for $[(C_6F_5)_3B–NO]^-$ ($S = 1$)

O	-1.02780368930644	1.24602096074674	0.24339333343688
F	0.35667627461406	3.53860168010484	-1.53396060346114
F	-0.34976710926785	6.11387049124928	-1.43012909678543
F	1.76497628679827	0.42648339447387	-2.05509364025164
F	3.30510838111718	-0.28113413975158	1.53995739088694
F	-0.44389291636132	2.32876783125336	2.87928689136009
F	3.95855189376608	2.92385159985879	1.34610692703754
F	0.06379532264580	7.57047896581891	0.83721392950743
F	1.32903975350211	-0.92362215568334	5.73118923408110
F	3.24992128116893	-1.51110029906439	3.89065751631860
F	4.07170826073302	0.20658878906356	-3.33902263502281
F	6.24290940511746	2.70898474350386	0.02316848357171
F	6.34582197296840	1.32435736434981	-2.35044068966654
F	1.21236751835204	6.38296760577594	3.01191396536345
F	1.90981265741896	3.82135407197222	2.94743578837539
F	-0.47977540511446	1.05614197844913	5.20458535129522
N	0.15785963702464	1.21532247455492	-0.08178999439783
C	2.35088263710387	0.11797029429450	2.41285226458998
C	5.13272351355739	2.15269698775587	-0.49205778715874
C	1.33071410056060	4.32309442102775	1.83567145326731
C	3.92475018418130	2.25810176907711	0.17125885435634
C	0.99157084063377	5.66672182258838	1.89496253214678
C	0.50039856181473	1.38374570312424	3.07024958178592
C	0.19826512075026	5.52903322738024	-0.34951881795804
C	2.33700761486044	-0.56071505671176	3.62379549286034
C	5.18824891888846	1.45414960538572	-1.68535174117901
C	1.45509946241000	1.13000258145134	2.08796112141477
C	2.73188739378612	1.70023931925663	-0.27501912763733
C	1.37466609045406	-0.25866501431177	4.56853166373892
C	1.09210948120362	3.51845805641435	0.72795466447415

C	0.55518201795037	4.18910868106075	-0.36660321720563
C	4.02808758533172	0.88865606487051	-2.18148471709086
C	2.83311810673811	1.02262607942974	-1.48418170566890
C	0.40986093555347	6.27483152614556	0.79675031191544
C	0.44897273539894	0.73059115969861	4.28822314471594
B	1.38507517364572	1.89532741538608	0.63245387698355

Optimized Coordinates for $[(C_6F_5)_3B–ON]^-$ ($S = 0$)

N	0.22387334634320	1.15509770869966	-1.19588812828523
F	0.53330155668843	3.82117163728540	-1.33811727961969
F	-0.27368943387993	6.31273649297425	-1.02926943535536
F	2.24681715778991	-0.49246463801973	-0.61147502607815
F	3.59453919861728	0.06734027635585	1.96866478025564
F	-0.63850597688055	2.15517457263370	2.54252607521959
F	3.84817349055151	3.89614608659411	0.20736801009832
F	0.09029916863966	7.60792992056007	1.35760151381375
F	0.83221984351046	-1.11023908156571	5.56111506406448
F	3.13256908692372	-1.40627951345060	4.13526788626857
F	4.16195892694429	-0.82615576594615	-2.45774827379914
F	5.79161881661909	3.50213250908037	-1.56494480399124
F	5.94633492087735	1.15811254381629	-2.95951891069786
F	1.26731724472144	6.29036075143122	3.43058394878004
F	2.03171662491664	3.74766440556072	3.17148781000705
F	-1.05214044522060	0.68721786671056	4.72848651358022
O	0.23982471817469	1.44890755070959	0.00382774885304
C	2.40834928729405	0.24983909974647	2.59194154358737
C	4.87540370317849	2.53846791318714	-1.36562153558145
C	1.43403100774496	4.32515448346341	2.10439884075122
C	3.84315391689371	2.71742801512582	-0.45601396259642
C	1.06138454210575	5.65104727251978	2.26586692638124
C	0.31952108936707	1.26633823716423	2.88293161958083
C	0.28712000194709	5.67431616754399	0.01201606725611
C	2.20433526861881	-0.52081875327212	3.72956822439220
C	4.97186219259465	1.34746018197119	-2.05861038324231
C	1.47644228807559	1.16396573747235	2.11499265074684
C	2.87268729696061	1.76302136429163	-0.19674636396621
C	1.03885626540753	-0.38060209788382	4.45603601181636
C	1.24305447070917	3.60937302637723	0.92735728540365
C	0.69204036730342	4.35512428465096	-0.11092876699807
C	4.05210485502838	0.34431063370412	-1.80490315559823
C	3.04193153495572	0.56258306163350	-0.88401224766201
C	0.46923238704380	6.33052095422547	1.21408017839557
C	0.08414056183706	0.52838185284655	4.02842582694732
B	1.58405071759724	2.02314524180209	0.74017374727183

Optimized Coordinates for $[(C_6F_5)_3B–ON]^-$ ($S = 1$)

N	-1.00747640807560	1.35640043794547	0.26421589661018
F	0.35056664723692	3.51650691584355	-1.53465416319189
F	-0.34962746306729	6.09736795982646	-1.45043567933449
F	1.75919336200483	0.41986502031814	-2.04648079486017
F	3.28692602560641	-0.28798785702377	1.52899866151648
F	-0.43281120003510	2.34120358661774	2.92044202678898
F	3.94805846139033	2.92314400539966	1.35465673792085
F	0.07959573465010	7.57144613442663	0.80064739622864
F	1.34157673354443	-0.94244910121491	5.73005372015944
F	3.24592749521074	-1.52765181740571	3.87065577134671
F	4.06361338656160	0.20945227078271	-3.33158945081006
F	6.23290623783360	2.71157038917179	0.03159607361133
F	6.33632506602654	1.32938678127031	-2.34380118649476
F	1.23083997188636	6.39902905685187	2.98156772898380
F	1.90515862462739	3.83119086503023	2.94213014367226
F	-0.46622199366922	1.04456217028132	5.22576456415144
O	0.21576758220416	1.20650019525734	-0.10125578265270
C	2.34206008488687	0.11322456669238	2.41059022534344
C	5.12333764081438	2.15483090839692	-0.48420090268531
C	1.32715156384865	4.32630381696113	1.82718099018503
C	3.91533482346586	2.25826118721713	0.17901862896152
C	0.99943325441763	5.67314964751659	1.87361392583972
C	0.50485943840582	1.38607147974985	3.09039011083687
C	0.19711676121035	5.51786917047265	-0.36650115544506
C	2.33527806048572	-0.57195987685919	3.61799482564432
C	5.17905819642253	1.45749452078873	-1.67812923386919
C	1.44790761950243	1.13017796951664	2.09746286660384
C	2.72285819801935	1.69903169848405	-0.26654105044789
C	1.38039730888602	-0.27223715329549	4.57076731561677
C	1.07882067400256	3.51233755310418	0.72904190991223
C	0.54647604305681	4.17566130739006	-0.37270094476315
C	4.01935777817329	0.89086730719049	-2.17378854607313
C	2.82402741544090	1.02126732251198	-1.47609023858935
C	0.41714738708567	6.27347723012140	0.77176767252905
C	0.45705835164012	0.72241362400652	4.30325255474126
B	1.37793113629862	1.89613070665491	0.64527938201287

Optimized Coordinates for *cis* $[(C_6F_5)_3B–ONNO]^-$ ($S = {}^1/_2$)

N	-1.00182844456360	1.59556408251511	0.10668420958307
F	0.37593370962614	3.60257772272287	-1.57146269294339
F	-0.34170615184746	6.16722488021674	-1.41186139019342
F	1.85908495759552	0.45495216142357	-2.12042131819327
F	3.23875603034344	-0.32006261204338	1.42223864254568

F	-0.47387584548611	2.30207849212618	2.85247143353745
F	3.92369406778592	2.96313286509713	1.35428502807270
F	0.04037246774282	7.57003689909009	0.89904076247018
F	1.27473806385254	-1.03827244295723	5.60690825698763
F	3.18250544984260	-1.60346854323779	3.73633041088140
F	4.19732776659862	0.28254300562675	-3.34562971973118
F	6.24929191676131	2.78091468013091	0.09061387812003
F	6.42589428557740	1.42030410290239	-2.29181812841051
F	1.16011802982810	6.32846648369121	3.05916290065541
F	1.86395592430308	3.77238984745689	2.93829538212554
F	-0.52323006123903	0.96124552919108	5.12610761260020
O	0.28637507575963	1.21677107551498	-0.23282002821714
C	2.29415666061815	0.07339792830211	2.30905524948578
C	5.15664357114098	2.21819057574036	-0.45663696245067
C	1.29942286085381	4.29982092787111	1.83044097534945
C	3.92953082146935	2.30391389572738	0.17536237577305
C	0.95663231311094	5.64106122446481	1.92026026903807
C	0.46349975528283	1.34192833738254	3.00440868231700
C	0.19557169255559	5.55950418632055	-0.33815799396814
C	2.27792768930198	-0.63715465396643	3.50186748613510
C	5.25137340014081	1.53215114570773	-1.65444053050377
C	1.41321720011557	1.10641361804175	2.01287487152553
C	2.75492533622372	1.73680114078507	-0.30667533216955
C	1.32156879326397	-0.35062010637713	4.45732196658399
C	1.07645142359478	3.52257302050615	0.69979852111054
C	0.55794412169984	4.22210839379987	-0.38503158972764
C	4.11195454497059	0.95760506944247	-2.18553832162994
C	2.89781514654902	1.06929669078829	-1.51861654449751
C	0.38881401222157	6.27617072714245	0.83000313046200
C	0.40438801859074	0.65264330418471	4.20273311458465
B	1.36723896649165	1.90444428050405	0.56460207105703
N	-1.82956212487539	0.82952154774207	-0.36700435863964
O	-1.75565144580155	-0.18812948357757	-1.06057231972577

Optimized Coordinates for *trans* $[(C_6F_5)_3B–ONNO]^-$ ($S = {}^1/_2$)

N	-1.04417903910901	1.58008139591226	0.49205658836193
F	0.29534106984507	3.51477726373524	-1.42533711605525
F	-0.36642779473036	6.10406440474700	-1.35189572398106
F	1.65005132890277	0.42344868389287	-1.97856814070054
F	3.30377195997482	-0.28094617997752	1.53400594731017
F	-0.36134929733542	2.31918234092842	3.13176033620642
F	3.91309257340965	2.92084872425839	1.38129591097003
F	0.10616759522451	7.58763748443061	0.88532372542065
F	1.57772004314612	-0.97965865167375	5.81569567280028
F	3.37480661234548	-1.54554249689186	3.84714500126253

F	3.92472221286640	0.20454284687934	-3.30444648311684
F	6.16651552541391	2.70674477347434	0.01203677226203
F	6.22382472172043	1.31802914672914	-2.36005304415117
F	1.27237984315954	6.41529552261630	3.05741544954781
F	1.90987873880990	3.83977791174052	3.03094623630312
F	-0.29485278247904	0.98329858367649	5.40103307045795
O	0.17859583355582	1.19834371301402	0.02738463115243
C	2.39448749132409	0.11041516824027	2.45790722552312
C	5.04655423144885	2.15095481710022	-0.48144385657931
C	1.32103973729757	4.33119630316818	1.91987623892381
C	3.85245034654992	2.25771489006476	0.20519159179052
C	1.01398783574939	5.68357045299955	1.95939748139464
C	0.58807789773532	1.36432930975167	3.23766570610041
C	0.18456336459457	5.52504502123578	-0.26957137912743
C	2.45178601140325	-0.58677458936095	3.65680492838841
C	5.07837086165788	1.45055160881227	-1.67437927982972
C	1.48067736488233	1.12543656386744	2.19526789692358
C	2.65027506707678	1.69959919770896	-0.21481227506862
C	1.54435006628239	-0.30326920126322	4.65913846568945
C	1.04937655313467	3.51276537554514	0.83075691865923
C	0.51514698626581	4.17863154507686	-0.26910427291053
C	3.90742593878568	0.88727355711762	-2.14644649064624
C	2.72603601426797	1.02279487953829	-1.42634669809347
C	0.42687565391603	6.28516261170366	0.86100566638849
C	0.59942750019892	0.68408192133065	4.44287444537262
B	1.32559285843451	1.88932848680782	0.73489151875001
N	-1.95276658674934	0.85455282961660	0.07108043887912
O	-3.16359433897741	0.92852378344636	0.25570689542127

Optimized Coordinates for $[(C_6F_5)_3B–NO_2]^-$ ($S = 0$)

N	0.09268638570557	0.05008882721981	-0.07126713394389
F	0.36726677178388	3.59115667103768	-1.49792240979943
F	-0.35383915058296	6.16025517622860	-1.38519550389713
F	1.54933290988204	1.07359175107171	-2.25389185614898
F	3.30250617398052	-0.23497426449510	1.67839277396215
F	-0.48356503288402	2.40064190928746	2.81718322497195
F	4.09523893074698	2.48244494725292	1.50403616480379
F	0.07284551422798	7.61638685570883	0.88023835049577
F	1.21048929893141	-0.75264472842382	5.82986950833508
F	3.18256021758974	-1.39641774052628	4.06267833438113
F	3.78559896592366	0.80971861430341	-3.64665675633194
F	6.33884562582424	2.18151361339260	0.07122132057104
F	6.21484595697561	1.33975451151617	-2.51698712211707
F	1.25456300216312	6.43449857833623	3.03944531730772
F	1.96676571408373	3.87467764668832	2.96514230385826

F	-0.57086337371764	1.21555190850735	5.20363585265077
O	-0.90639534406775	-0.35583155028923	-0.58764221967040
O	0.11679272103330	1.39319955794413	0.01331322258502
C	2.33413086242639	0.19652879276567	2.51619911585207
C	5.14549670601875	1.91610266241082	-0.48885560085317
C	1.37434222194556	4.37658092297264	1.85988384778566
C	3.97126078212741	2.05124967681220	0.22857200415158
C	1.02809154050545	5.71881968592670	1.92394167603818
C	0.46738887403311	1.47812753535894	3.08355585002695
C	0.20559729589823	5.57729153705838	-0.30980971348247
C	2.28269822382686	-0.44913552780571	3.74457973801719
C	5.08841303400278	1.48463940714522	-1.80340362814671
C	1.45058063194665	1.19856102966564	2.13838300428618
C	2.71001352636707	1.74804207420362	-0.27343838470184
C	1.29515924155541	-0.11825830323954	4.65282683906663
C	1.11583005387076	3.56869621253002	0.75937137367541
C	0.56802273270341	4.23902300952939	-0.33165349871705
C	3.85581484381626	1.21213754213448	-2.36575419914827
C	2.70076349499182	1.35140321109919	-1.60568000131450
C	0.42624527832206	6.32335089122543	0.83462447006183
C	0.38014810357147	0.86497673371701	4.32027223376797
B	1.38512726447109	1.94583062172902	0.67402150162051

Optimized Coordinates for N_2O ($S = 0$)

N	0.00000	0.00000	0.00000
N	0.00000	0.00000	-1.11957
O	0.00000	0.00000	1.18450

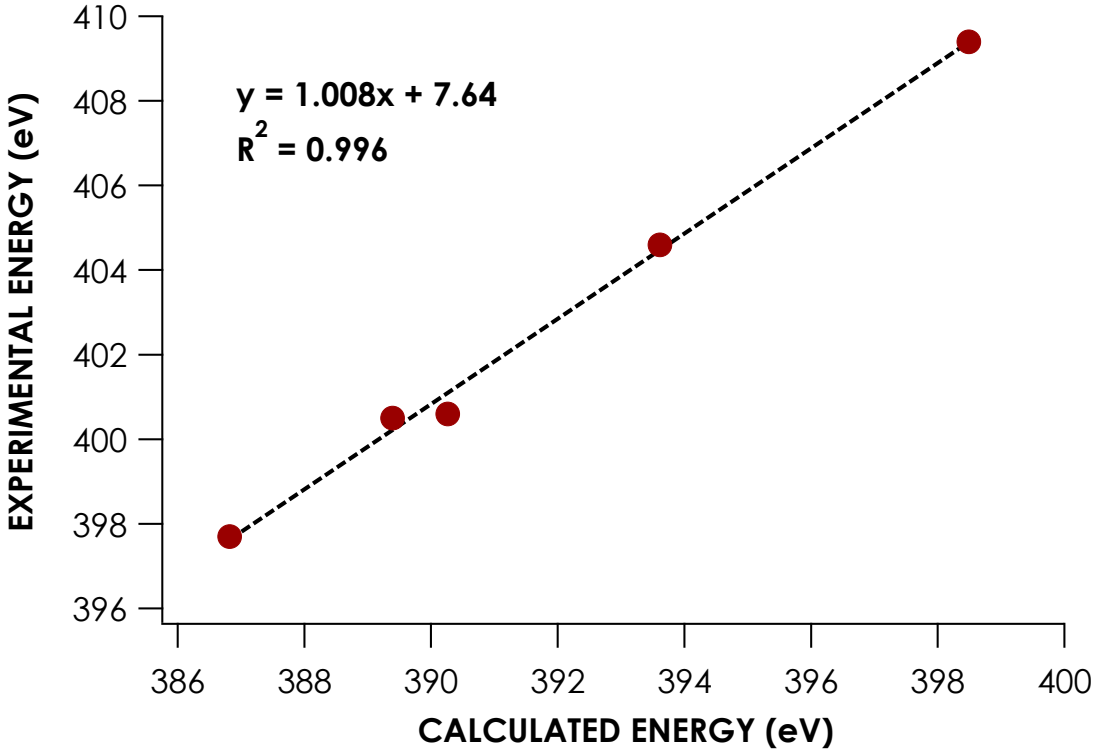

Figure 41. Correlation of experimental and calculated N K-edge peak energies for **3** and **4**.

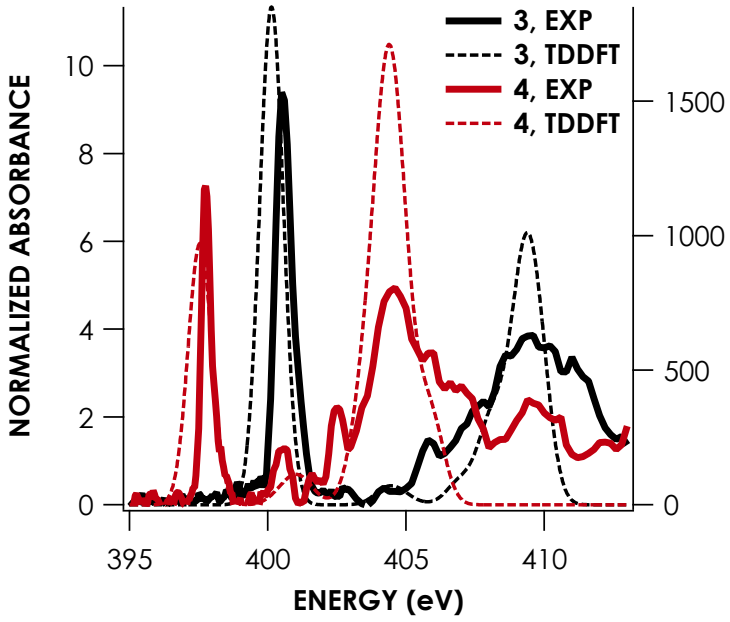

Figure 42. Overlay of smoothed experimental PFY N K-edge XAS of **3** and **4** (solid lines) with TDDFT-calculated spectra (dashed lines).

18. References for Supplementary Information

1 Weston Jr., R. E. & Brodasky, T. F. Infrared Spectrum and Force Constants of the Nitrite Ion. *J. Chem. Phys.* **27**, 683-689 (1957).

2 Miller, F. A. & Wilkins, C. H. Infrared Spectra and Characteristic Frequencies of Inorganic Ions. *Anal. Chem.* **24**, 1253–1294 (1952).

3 Kundu, S. *et al.* Nitrosyl Linkage Isomers: NO Coupling to N_2O at a Mononuclear Site. *J. Am. Chem. Soc.* **141**, 1415-1419 (2019).

4 Ghosh, P. *et al.* NO Coupling at Copper to *cis*-Hyponitrite: N_2O Formation via Protonation and H-atom Transfer. *J. Am. Chem. Soc.* **144**, (2022) doi: 10.1021/jacs.2c04033.

5 Wright, A. M., Wu, G. & Hayton, T. W. Formation of N_2O from a Nickel Nitrosyl: Isolation of the cis-$[N_2O_2]^{2-}$ Intermediate. *J. Am. Chem. Soc.* **134**, 9930−9933 (2012).

6 Mokhtarzadeh, C. C., Chan, C., Moore, C. E., Rheingold, A. L. & Figueroa, J. S. Side-On Coordination of Nitrous Oxide to a Mononuclear Cobalt Center. *J. Am. Chem. Soc.* **141**, 15003−15007 (2019).

7 Zhang, S., Melzer, M. M., Sen, S. N., Çelebi-Ölçüm, N. & Warren, T. H. A motif for reversible nitric oxide interactions in metalloenzymes. *Nature Chem.* **8**, 663-669 (2016).

8 Titus, C. J. *et al.* L-Edge Spectroscopy of Dilute, Radiation-Sensitive Systems Using a Transition-Edge-Sensor Array. *J. Chem. Phys.* **147**, 214201-214207 (2017).

9 Fowler, J. W. *et al.* The practice of pulse processing. *J. Low Temp. Phys.* **184**, 374-381 (2016).

10 Solé, V. A., Papillon, E., Cotte, M., Walter, P. & Susini, J. A multiplatform code for the analysis of energy-dispersive X-ray fluorescence spectra. *Spectrochim. Acta. B* **62**, 63-68 (2007).

11 Stoll, S. & Schweiger, A. EasySpin, a comprehensive software package for spectral simulation and analysis in EPR. *J. Magn. Reson.* **178**, 42-55 (2006).

12 Neese, F. The ORCA program system. *WIREs Comput. Mol. Sci.* **2**, 73-78 (2012).

13 DeBeer George, S., Petrenko, T. & Neese, F. Prediction of Iron K-Edge Absorption Spectra Using Time-Dependent Density Functional Theory. *J. Phys. Chem. A.* **112**, 12936−12943 (2008).

14 Stephens, P., Devlin, F., Chabalowski, C. & Frisch, M. J. Ab Initio Calculation of Vibrational Absorption and Circular Dichroism Spectra Using Density Functional Force Fields. *J. Phys. Chem. A* **98**, 11623−11627 (1994).

15 Weigend, F. & Ahlrichs, R. Balanced basis sets of split valence, triple zeta valence and quadruple zeta valence quality for H to Rn: Design and assessment of accuracy. *Phys. Chem. Chem. Phys.* **7**, 3297−3305 (2005).

16 Weigend, F. & Ahlrichs, R. Balanced Basis Sets of Split Valence, Triple Zeta Valence and Quadruple Zeta Valence Quality for H to Rn: Design and Assessment of Accuracy. *Phys. Chem. Chem. Phys.* **7**, 3297-3305 (2005).

17 Pantazis, D. A., Chen, X.-Y., Landis, C. R. & Neese, F. All-Electron Scalar Relativistic Basis Sets for Third-Row Transition Metal Atoms. *J. Chem. Theory Comput.* **4**, 908−919 (2008).

18 van Lenthe, E., van der Avoird, A. & Wormer, P. E. S. Density functional calculations of molecular hyperfine interactions in the zero order regular approximation for relativistic effects. *J. Chem. Phys.* **108**, 4783−4796 (1998).

19 van Wüllen, C. Molecular density functional calculations in the regular relativistic approximation: Method, application to coinage metal diatomics, hydrides, fluorides and chlorides, and comparison with first-order relativistic calculations. *J. Chem. Phys.* **109**, 392−399 (1998).

20 F. Neese, F. Wennmohs, A. Hansen & Becker, U. Efficient, Approximate and Parallel Hartree–Fock and Hybrid DFT Calculations. A 'Chain-of-Spheres' Algorithm for the Hartree–Fock Exchange. *Chem. Phys.* **356**, 98-109 (2009).

21 Neese, F. Prediction and Interpretation of the 57Fe Isomer Shift in Mössbauer Spectra by Density Functional Theory. *Inorganica Chim. Acta* **337**, 181-192 (2002).
22 Klamt, A. & Schüürmann, G. COSMO: A New Approach to Dielectric Screening in Solvents with Explicit Expressions for the Screening Energy and Its Gradient. *J. Chem. Soc., Perkin Trans.* **2**, 799-805 (1993).
23 Lukens, J. T., DiMucci, I. M., Kurogi, T., Mindiola, D. J. & Lancaster , K. M. Scrutinizing metal–ligand covalency and redox non-innocence via nitrogen K-edge X-ray absorption spectroscopy. *Chem. Sci.* **10**, 5044–5055 (2019).
24 Neese, F. Metal and ligand hyperfine couplings in transition metal complexes: The effect of spin–orbit coupling as studied by coupled perturbed Kohn–Sham theory. *J. Chem. Phys.* **118**, 3939-3948 (2003).
25 Schlegel, H. B. In: Lawley, K. P. (editor), *Advances in Chemical Physics: Ab initio methods in quantum chemistry, Part I*, Vol. 67, p. 249 (John Wiley and Sons, 2009).
26 Schlegel, H. B. In: Yarkony, D. R. (editor), *Modern Electronic Structure Theor*y, Vol. 459, (World Scientific, 1995)
27 Schlegel, H. B. In: v. R. Schleyer, P. (editor), *Encyclopedia of Computational Chemistry,* p. 1136, (John Wiley and Sons, 1998).
28 Eckert, F.; Pulay, P.; Werner, H. J. *Ab initio* geometry optimization for large molecules. *J. Comput. Chem.* **12**, 1473-1483 (1997).
29 Horn, H.; Wei, H.; Háser, M.; Ehrig, M.; Ahlrichs, R. Prescreening of two-electron integral derivatives in SCF gradient and Hessian calculations. *J. Comput. Chem.* **12**, 1058-1064 (1991).
30 Baker, J. An algorithm for the location of transition states. *J. Comput. Chem.* **7**, 385-395 (1986).
31 Hess, B.; Kutzner, C.; van der Spoel, D.; Lindahl, E. GROMACS 4: Algorithms for Highly Efficient, Load-Balanced, and Scalable Molecular Simulation. *J. Chem. Theory Comput*. **4,** 435-447 (2008).
33 Harvey, J. N.; Aschi, M.; Schwarz, H.; Koch, W. The singlet and triplet states of phenyl cation. A hybrid approach for locating minimum energy crossing points between non-interacting potential energy surfaces. Theor. Chem. Acc. **99**, 95-99 (1998).
33 Li, H.; Jensen, J. H. Partial Hessian vibrational analysis: the localization of the molecular vibrational energy and entropy. *Theor. Chem. Acc.* **107**, 211-219 (2002).